

# Improved representation of soil moisture processes through incorporation of cosmic-ray neutron count measurements in a large-scale hydrologic model

Eshrat Fatima<sup>1,2</sup>, Rohini Kumar<sup>1</sup>, Sabine Attinger<sup>1,2</sup>, Maren Kaluza<sup>1</sup>, Oldrich Rakovec<sup>1,3</sup>, Corinna Rebmann<sup>1</sup>, Rafael Rosolem<sup>4</sup>, Sascha Oswald<sup>2</sup>, Luis Samaniego<sup>1,2</sup>, Steffen Zacharias<sup>5</sup>, and Martin Schrön<sup>5</sup>

<sup>1</sup>Dep. Computational Hydrosystems, UFZ - Helmholtz Centre for Environmental Research GmbH, Leipzig, Germany

<sup>2</sup>Institute of Environmental Science and Geography, University of Potsdam, Potsdam, Germany

<sup>3</sup>Faculty of Environmental Sciences, Czech University of Life Sciences Prague, Praha-Suchdol 16500, Czech Republic

<sup>4</sup>Department of Civil Engineering, University of Bristol, Bristol

<sup>5</sup>Dep. Monitoring and Exploration Technologies, UFZ - Helmholtz Centre for Environmental Research GmbH, Leipzig, Germany

**Correspondence:** Eshrat Fatima (eshrat.fatima@uni-potsdam.de), Rohini Kumar (rohini.kumar@ufz.de), Martin Schrön (martin.schroen@ufz.de)

**Abstract.** Profound knowledge of soil moisture and its variability plays a crucial role in hydrological modeling to support agricultural management, flood and drought monitoring and forecasting, and groundwater recharge estimation. Cosmic-ray neutron sensing (CRNS) has been recognized as a promising tool for soil moisture monitoring due to its hectare-scale footprint and decimeter-scale measurement depth. But since CRNS provides an integral measurement over several soil horizons, a direct comparison of observed and simulated soil moisture products is not possible. This study establishes a framework to assess the accuracy of soil moisture simulated by the mesoscale Hydrological Model (mHM) by generating and comparing simulated neutron counts with observed neutron measurements for the first time. We included three different approaches to estimate CRNS neutron counts in mHM as a function of the simulated soil moisture profiles: two methods based on the Desilets equation and one based on the forward operator COSMIC (Cosmic-ray Soil Moisture Interaction Code). For the Desilets method we tested two different approaches to average the vertical soil moisture profiles: a uniform vs. a non-uniform weighting scheme depending on the CRNS measurement depth. The methods were tested at two agricultural sites, one pasture site, and one forest site in Germany. To explore the prior and posterior distributions of the mHM parameters when constrained by CRNS observations, we used a Monte Carlo method based on Latin hypercube sampling with a large sample size ( $S = 100\,000$ ). We found that all three methods performed well with Kling-Gupta efficiency  $> 0.75$  and percent bias  $< \pm 10\%$  across the majority of investigated sites and for the best 1% of parameter sets. The performance of the neutron forward models varied slightly across different land cover types. The non-uniform approach generally showed good performance, particularly at the agricultural sites. While the COSMIC method performed slightly better at the forest site. The uniform approach showed slightly better results at the grassland site. We also demonstrated for the first time that the incorporation of CRNS measurements into mHM could improve both, the soil moisture and the evapotranspiration products of mHM. This suggests that CRNS is capable

20 of improving the model parameter space in general and adds a broader perspective on the potential of CRNS to support large-scale hydrological and land surface models.

## 1 Introduction

Soil moisture is a key terrestrial climate variable because it controls the mass and energy exchange between the Earth's surface, the groundwater, the vegetation, and the atmosphere. Understanding soil moisture levels with changes in temperature is crucial for enhancing the predictability of climate patterns on inter-seasonal and annual time scales, as highlighted in previous studies (Santanello Jr et al., 2011; Seneviratne et al., 2006). Moreover, soil moisture variability also plays a significant role in a wide range of applications, including flood forecasting, weather forecasting, climate modeling, agricultural management, and groundwater recharge (Van Steenberghe and Willems, 2013; Albergel et al., 2010; Jablonowski, 2004; Wahbi et al., 2018; Samaniego et al., 2019; Barbosa et al., 2021). In hydrological modeling, soil moisture is a key variable controlling the partitioning of precipitation into evapotranspiration, infiltration, and runoff (Fuamba et al., 2019; Zhuo et al., 2020). Proper initialization and modeling of soil moisture are crucial for predicting other hydrologic processes (e.g., runoff, evapotranspiration, etc). Nevertheless, uncertainties in input data and model parameters, along with limitations in the representation of subsurface processes, can impede the reliability of soil moisture estimation (Chen et al., 2011). Obtaining accurate soil moisture measurements at a field scale is challenging due to current measurement limitations and subsurface complexity (Dong and Ochsner, 2018). Estimating average soil moisture at a mesoscale ( $\approx 1\text{--}100$  km) is particularly difficult due to measurement technique limitations in terms of their "footprint" and measurement methods to bridge the scale gap between point-scale and areal average measurements for hydrologic modeling (Chan et al., 2018).

One promising approach to infer soil moisture at a field scale is the cosmic-ray neutron sensing (CRNS) technique (Zreda et al., 2008; Desilets et al., 2010; Zreda et al., 2012a). It is based on a neutron detector that counts the average number of neutrons in the air above the ground which represents the average hydrogen content in the environment. The method has demonstrated potential for estimating average soil moisture over areas of several hectares in size and tens of decimeters in-depth (Köhli et al., 2015; Schrön et al., 2017). CRNS probes are typically calibrated locally using soil samples within their support volume (Franz et al., 2012; Schrön et al., 2017). CRNS data are used in various studies, including land surface modeling, vegetation dynamics, catchment hydrology, and supporting the agriculture sector with soil and climate data (Franz et al., 2020). Moreover, CRNS derived soil moisture has been valuable in water balance studies, aiding in estimating infiltration and evapotranspiration (Schreiner-McGraw et al., 2015; Foolad et al., 2017; Wang et al., 2018).

When it comes to the comparison of observed CRNS soil moisture with the results from a hydrological model, a major challenge is to select the right vertical scale. A CRNS measurement is an integral value over a measurement volume, and the depth of this volume depends on the soil moisture profile in a non-linear way (Köhli et al., 2015). While it is well understood in which depth the measured neutrons probed the soil, it is not directly clear how to compare the CRNS soil moisture product with several soil layers in a model. Shuttleworth et al. (2013) argued that the direct comparison of the raw product – the neutron counts – would be the favorable way to compare simulations with observations instead. By simulating neutrons directly, one

could emulate the neutron counts per grid cell based on its soil moisture profile in the model, and then compare the result directly with the corresponding neutron measurement.

55 One way to calculate neutrons within the model is to use established empirical relationships between average soil moisture and neutrons (Desilets et al., 2010; Köhli et al., 2021). Another way is to employ the neutron forward operator COSMIC (Cosmic-ray Soil Moisture Interaction Code) introduced by (Shuttleworth et al., 2013). It emulates the effective vertical neutron transport through the soil and thereby enables a comprehensive representation of the neutron generation process. Although this operator can only be a simplification of the actual physical processes as modeled by, e.g., URANOS (Köhli et al., 2023), its  
60 higher complexity still comes with higher computational demand compared to the mentioned analytical relationships.

Previous studies, such as Barbosa et al. (2021) and Brunetti et al. (2019), have recognized the importance of CRNS over traditional invasive point-scale techniques and have utilized the HYDRUS-1D model to simulate soil moisture at the field scale. HYDRUS-1D offers a valuable framework for modeling soil moisture dynamics and has been particularly addressing the subsurface processes. These studies incorporated a neutron forward operator COSMIC to simulate the neutron counts  
65 based on soil moisture profiles. They inversely calibrated soil hydraulic parameters by comparing observed and simulated neutron count rates, whereas beforehand this was limited to be done via comparison of depth-averaged soil moisture values (Rivera Villarreyes et al., 2014). The potential utility of using CRNS data to calculate volumetric soil water content (SWC) and improve soil hydraulic parameters within land surface models has also been observed earlier, as highlighted by Rosolem et al. (2014). In Iwema et al. (2017), a Land Surface Model investigated the impact of reducing scale mismatch between energy  
70 flux and soil moisture observations using CRNS data. Patil et al. (2021) employed a distributed Land Surface Model, Data Assimilation Research Testbed (DART) with CRNS time series, and Ensemble Adjustment Kalman Filter to simulate water and energy balance. Both studies focused on analyzing land surface water and energy balance, exploring data assimilation and calibration techniques.

The Hydrologiska Bryans Vattenbalansavdelning (HBV) model, as studied by Dimitrova-Petrova et al. (2020), employed  
75 CRNS data in a mixed-agricultural landscape to explore water balance on the land surface. While, Beck et al. (2021) used remote sensing products and groundwater level measurements to temporally calibrate the HBV model, emphasizing the challenge of comparing satellite-derived soil moisture with point-scale in-situ measurements. Additionally, Baatz et al. (2017) was the first study that utilized spatially distributed hydrological modeling, integrating CRNS data, FAO and BK50 soil maps, and other soil data in the Community Land Model (CLM). They demonstrated that assimilating CRNS data improved catchment-scale  
80 soil water content characterization by updating spatially distributed soil hydraulic parameters. Furthermore, Zhao et al. (2021) assessed the significance of CRNS data in CLM version 3.5, conducting simulations based on 13 CRNS stations over 2017-2018. Despite employing a simplified Richards equation, limitations included the absence of lateral flows and groundwater representation.

The mesoscale Hydrological Model (Samaniego et al., 2010b; Kumar et al., 2013b, mHM;) is known for its spatially distributed hydrologic predictions at a large scale incorporating with the multiscale parameter regionalization (MPR) technique. We chose the mHM in this study for its efficient parameterization approach that allows for a seamless prediction of water fluxes  
85 at different spatial resolutions (Samaniego et al., 2017; Zink et al., 2017; Jing et al., 2018; Schweppe et al., 2022). This feature

allows the model to scale its applications from a locally relevant scale to regional and continental scales (Kumar et al., 2013b; Huang et al., 2017; Rakovec et al., 2019). One of promising application of mHM is the operational German Drought Monitor (GDM) that provides daily updates on the soil moisture related drought status (Samaniego et al., 2013; Moravec et al., 2019; Pohl et al., 2023). Previous evaluation of the GDM for soil moisture focuses on assessing the skill of the model in reproducing SM anomalies based on point scale soil moisture observations (Zink et al., 2016, 2018; Rakovec et al., 2022; Scharnweber et al., 2020; Boeing et al., 2022). Such a evaluation is fraught with uncertainties due to scale mismatch between limited point scale observations versus grid-scale modeled estimates. In contrast, CRNS has been recognized as a promising tool for soil moisture monitoring due to its hectare-scale footprint and decimeter-scale measurement depth. Therefore, by including a CRNS neutron count framework within the mHM, it could better handle the scale mismatch issue and represent the soil moisture dynamics. The wide-spread availability of observed CRNS data opens up new opportunities to develop and implement novel methods and hypotheses to improve soil moisture representation in hydrologic models.

In this study, we established a framework to incorporate CRNS data into the mesoscale Hydrological Model (mHM) to compare empirical and forward-modeling approaches for neutron count estimation to improve soil water content parameters in mHM across different vegetation types in Germany. To do this, we compared modelled with measured neutron counts to infer optimal model parameters, such as soil hydraulic conductivity. Here, we test three approaches, (i) the direct calculation of neutrons from the equal-averaged SWC profiles based on Desilets et al. (2010), (ii) the same with weighted-average soil moisture profiles based on Schrön et al. (2017), and (iii) the neutron forward operator COSMIC by Shuttleworth et al. (2013). We evaluate the simulation of neutron counts at scales of  $1.2 \text{ km} \times 1.2 \text{ km}$ , comparing the results to observed neutron counts from three different sites including agriculture, deciduous forests, and grasslands. The goal of this study is to investigate the potential of using CRNS probes and measured neutron counts to improve soil moisture predictions through simulations in mHM across different land covers and soil properties and to evaluate the feasibility of incorporating neutron count measurements into the modeling scheme. We employ a (calibration) framework by applying a Monte Carlo experiment to account for parameter uncertainties. We further cross-evaluate our simulations and test the reliability of the CRNS incorporated soil-moisture scheme in mHM for simulating other variables by utilising time series of observed evapotranspiration from an eddy covariance station available. Finally, we discuss and provide guidelines (challenges and limitations) for incorporating CRNS measurements in a large-scale hydrologic model. In summary, the present paper aims to answer the following research questions:

- What is the best approach to simulate CRNS neutron counts in a hydrological model considering the heterogeneity of vertical soil moisture profiles?
- What is the impact of model calibration with CRNS observations on simulated evapotranspiration at Hohes Holz?
- Is the mHM at approx. 1 km resolution capable of capturing the dynamics of hectare-scale CRNS measurements at different landcover sites in a grid including 2 agriculture sites, 1 forest site, and 1 meadow site?

## 2 Materials and Methods

### 120 2.1 Experimental Site Description

For this study, we select four sites with CRNS sensors, namely *Grosses Bruch*, *Hohes Holz*, *Hordorf*, and *Cunnersdorf* in Northern Germany, as provided already within COSMOS EU (Bogena et al., 2022) with particularly long time series and with different land cover, i.e., agriculture, forest, and meadow (see Tab. 1). The first three sites belong to the TERENO observatory “Harz/Central Germany lowland” (Zacharias et al., 2011) while the fourth site is part of an agricultural research farm operated  
125 by the German Weather Service (DWD). The *Grosses Bruch* site is a meadow/grassland that is usually flooded naturally once or twice a year. The meadows have sandy loam fluvisol-gleysol soil, which is 1.5 meters deep and partially covered with a layer of peat (Wollschläger et al., 2017). Meteorological conditions like soil moisture and temperature at various depths are continuously monitored by a wireless soil moisture monitoring network (Schrön, 2017). *Hohes Holz* is a deciduous forest site and the performance of the CRNS sensor there is highly dependent on dynamic effects such as tree canopy water or seasonal  
130 fluctuations in wet biomass. Water trapped in leaves and litter can present a particular challenge for CRNS measurements, especially at forest stations (Bogena et al., 2013). Also, Bogena et al. (2022) indicated that the influence of seasonal changes of biomass on the CRNS signal is much less important than the influence of changing soil moisture, even in *Hohes Holz*, as changes in soil moisture are the much larger source of variation represented by the CRNS measurements. The mean annual air temperature for each site ranges from 10.0 to 10.9 °C and the average yearly precipitation ranges from 458 to 535 mm.

**Table 1.** Geographical characteristics of study sites: Site Names, Geographic Coordinates, Climatic Data (Annual Precipitation in mm/year, Annual Mean Temperature in °C), and the Periods Covered in Observed and Simulated Datasets.

Site	Latitude [°N]	Longitude [°E]	Altitude [m]	Land Cover	Precipitation [mm/year]	Temperature [°C]	Period
<i>Grosses Bruch</i>	52.02	11.10	80	Pasture, grassland	458	10.1	24/06/2014–31/01/2021
<i>Hohes Holz</i>	52.09	11.22	217	Forest, hilltop	469	10.3	27/08/2014–31/01/2021
<i>Hordorf</i>	51.99	11.17	82	Cropland	463	10.3	29/09/2016–31/01/2021
<i>Cunnersdorf</i>	51.36	12.55	140	Cropland	535	10.9	23/06/2016–31/01/2021

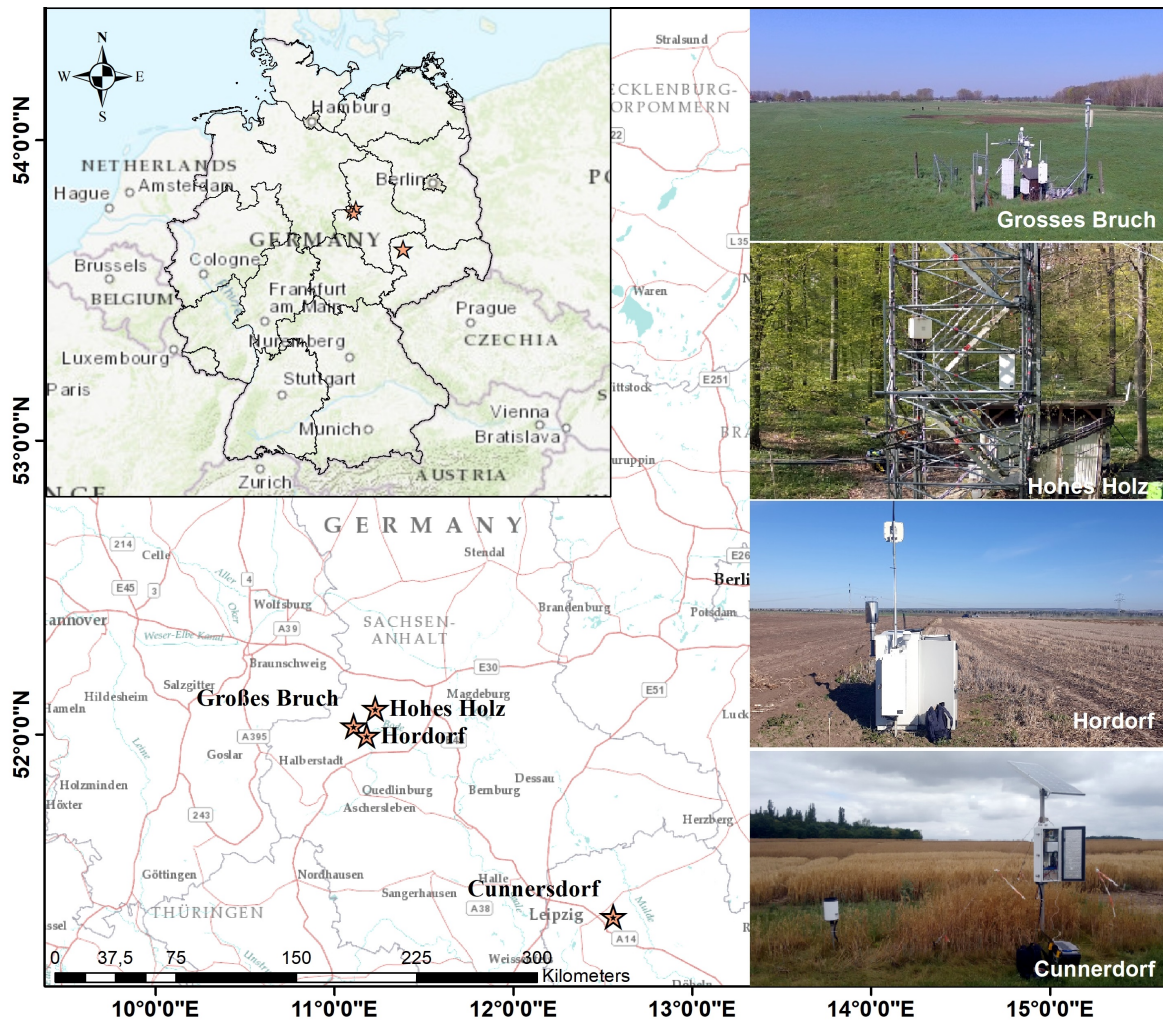


**Figure 1.** Study area map of Germany, highlighting the four test sites where observed neutron count rates from CRNS are utilized to evaluate the performance of mHM. The figure utilizes OSM basemap layers from (© OpenStreetMap contributors 2021; distributed under the Open Data Commons Open Database License (ODbL) v1.0) OpenStreetMap contributors (2020).

## 135 2.2 The mesoscale Hydrological Model (mHM)

mHM is a spatially distributed process-based hydrologic model capable of representing processes such as canopy interception, snow accumulation and melting, soil moisture dynamics, infiltration and surface runoff, evaporation, underground storage, and runoff generation, deep infiltration and baseflow, as well as runoff attenuation and flood routing (Samaniego et al., 2010a; Kumar et al., 2013a). The mHM is flexible for hydrological simulations at different spatial scales due to its novel Multi-scale  
 140 Parameter Regionalization approach (MPR; Samaniego et al., 2010b); and has demonstrated applicability in diverse settings

(Samaniego et al., 2010a; Kumar et al., 2013a; Rakovec et al., 2016a; Samaniego et al., 2017). The MPR's basic concept is to estimate parameters (e.g., porosity) based on soil properties (e.g., sand and clay content) using transfer functions at a fine spatial resolution (e.g. 100 m) and upscaling them to modelling resolutions (e.g., 1 km). In MPR, transfer functions (e.g., pedo-transfer functions to estimate soil parameters) are combined with morphological inputs (e.g., soil texture properties) and thus  
145 lead to model hydrologic parameters (e.g., porosity or hydraulic conductivity of the soil) (Livneh et al., 2015; Zacharias and Wessolek, 2007). In mHM, the soil moisture horizons/profile can be divided into several horizons, all of which are sensitive to root water uptake and evapotranspiration processes. mHM simulates the daily dynamics of soil moisture at different depths considering the incoming water (e.g., rainfall plus snow melt for the topmost layer and infiltration from above layers for other layers) and outgoing ET and ex-filtration fluxes. Further details on mHM code can be found at <https://mhm-ufz.org>.

### 150 2.3 Model Set-up

The latest version 5.12 of mHM is used in this study (see Samaniego et al., 2023, and <https://github.com/mhm-ufz>). The model was set up for a period of six years (2014–2020) with a daily time step, and the spatial resolution of the mHM grid cells was fixed at:  $0.01562^\circ \times 0.01562^\circ$  ( $\sim 1.2 \text{ km} \times 1.2 \text{ km}$  using the WGS84 coordinate systems). In mHM, Level 1 (L1) denotes the spatial resolution at which dominant hydrological processes are modelled and Level 2 (L2) denotes the resolution  
155 of the meteorological forcing data. The finest resolved spatial level L0 ( $0.001953125^\circ \times 0.001953125^\circ$ ) denotes the subgrid variability of relevant basin characteristics, which includes information on the soil as well as land use, topography, and geology.

Figure 2 shows the flow diagram depicting the basic methodology of our study, which includes the calculation of CRNS neutron count rates based on daily soil moisture values simulated with mHM. The model boundary conditions such as precipitation and temperature for the mHM are acquired from the German Weather Service (DWD) station closest to the test site. The potential evapotranspiration required by mHM is estimated using the Hargreaves-Samani method (Hargreaves and Samani, 1985).  
160 The model setup and parameterization for the soil moisture module use the scheme optimized by Boeing et al. (2022). A raster dataset describing the distribution of the soils in the model area and a corresponding lookup table with the attributes depth, soil texture (sand and clay fraction), and bulk density are required as soil input data and are derived from national digital soil maps provided by the Federal Institute for Geosciences and Natural Resources (BGR, 2020). The data set contains physical and  
165 chemical properties for soil at different layers and the available at a resolution of 1:250,000 (BUEK 200; BGR, 2020). mHM uses three dominant land cover classes (forest, permeable, and impervious) that were retrieved by a GLOBCOVER database ESA (2009). Furthermore, vegetation characteristics like Leaf Area Index (LAI) and fraction of roots for different vegetation types are prescribed in the model. The mHM soil domain is divided into three horizons with depths of 0–5 cm, 5–25 cm, and 25–60 cm. The upper two model layers are parameterized using the topsoil layer properties while for the lower model layer,  
170 the subsoil properties are used. More details on the underlying input data for mHM can be obtained from Boeing et al. (2022). In our study, we utilized three distinct modules of parameters: snow, soil moisture, and neutrons, with a total of 28 parameters employed for the Desilets method and 30 parameters for the COSMIC method. The simulation of soil water content is processed through these three modules to estimate neutron counts. To comprehensively cover the parameter set ranges, we em-

ployed 100 000 iterations. Finally, we selected the top 10 optimized parameter sets based on the objective function,  $KGE_{\alpha\beta}$ ,  
 175 for further analysis and evaluation.

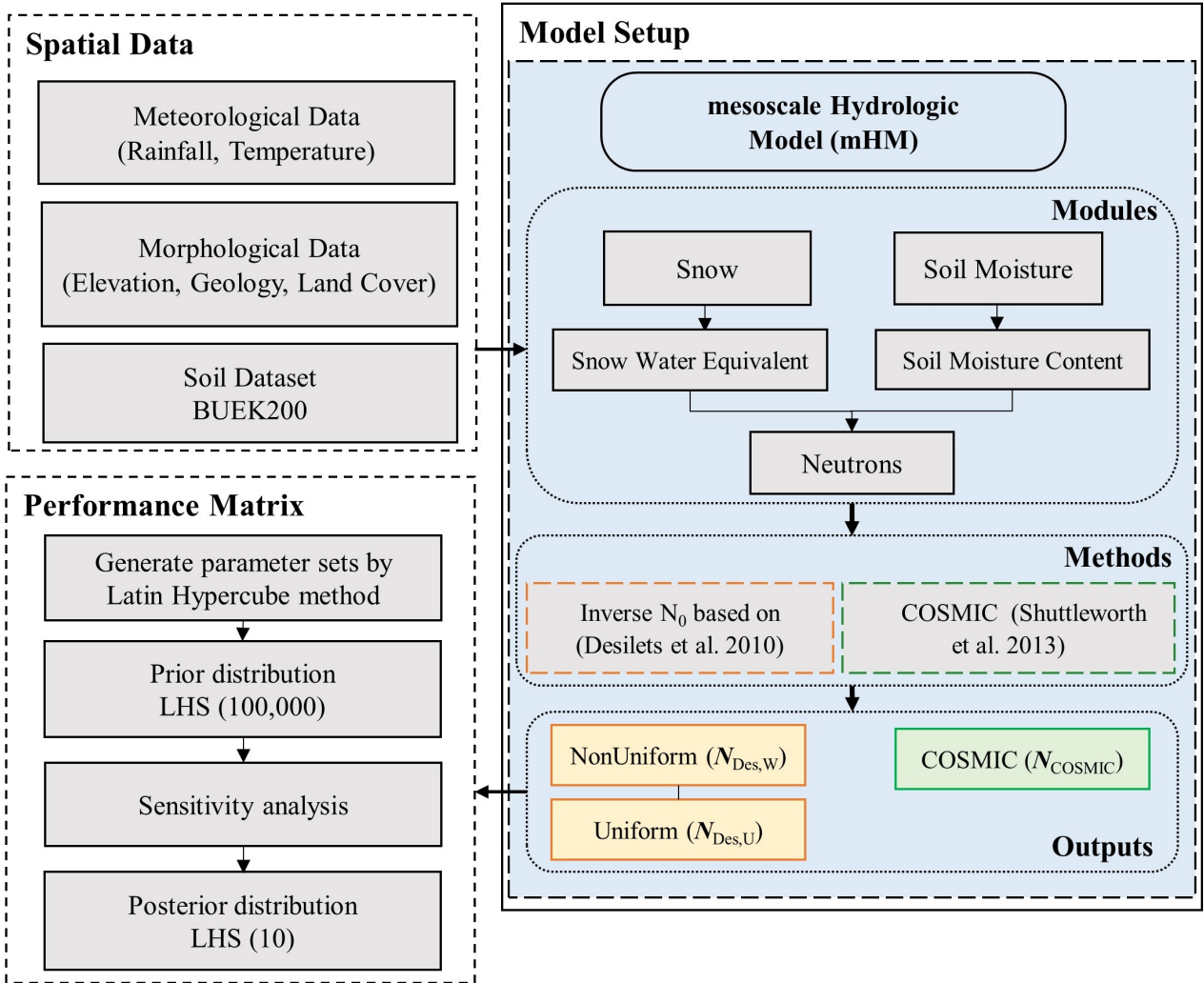


**Figure 2.** Flowchart depicting the methodology employed for calculating CRNS neutron counts through the utilization of the LHS technique for parameterization in mHM. The computation of CRNS neutron count is carried out through three distinct approaches:  $N_{Des,U}$ ,  $N_{Des,W}$ , and  $N_{COSMIC}$ .

## 2.4 Conversion of soil moisture to neutron count rate

In this study, we compared observed neutron counts from CRNS data with simulated neutron counts estimated from modeled soil moisture with the goal of optimizing the parameterization of soil water content from mHM shown in Fig. 3. By incorporat-



ing the approaches from Desilets et al. (2010) and Shuttleworth et al. (2013) directly into the mHM, we are able to account also  
 180 for the uncertainty in the model predictions and test their feasibility across four distinct sites. We analyzed the soil water content data at different soil layers (0–5 cm, 5–25 cm, and 25–60 cm) in mHM, as utilized in the study by Boeing et al. (2022). The accuracy of numerical calculations would benefit from higher resolved soil profiles, however, our experiments demonstrated that varying soil depths from 3 to 6 layers did not have a substantial impact on the simulated neutron count results in mHM. We used BGR (2020) which is a global dataset that is not detailed enough to allow for finer vertical resolution. Our main objective  
 185 is to optimize the parameterization of soil hydraulic properties in mHM based on the comparison between measurement and modelled neutron counts.

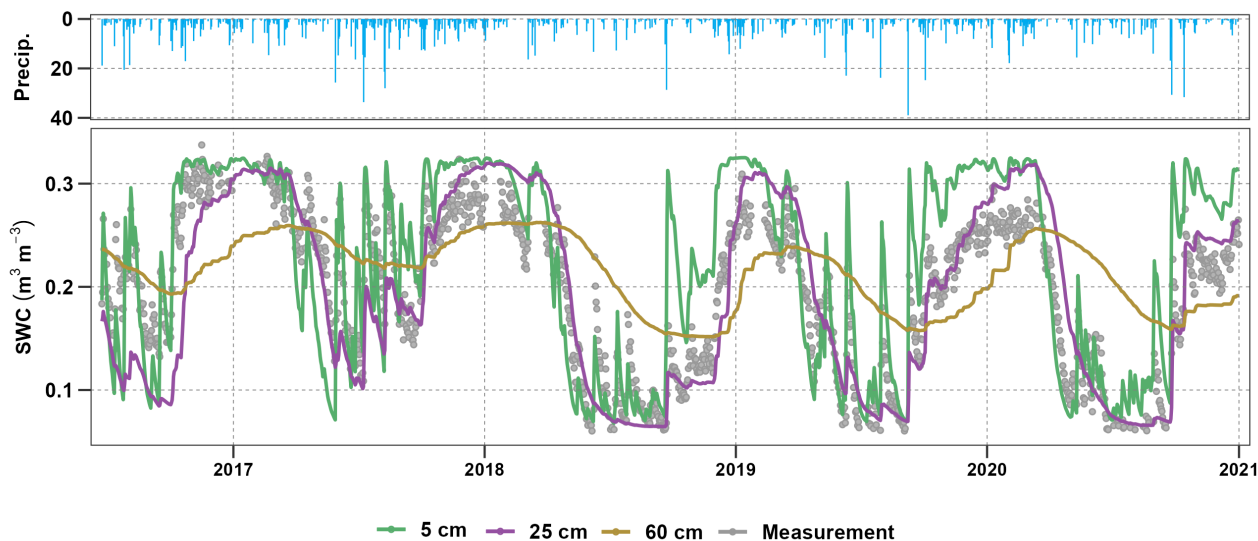


**Figure 3.** Daily time series of soil water content ( $\text{cm}^3 \text{cm}^{-3}$ ) at the *Cunnersdorf* site. The graph shows a comparison between the measured SWC from CRNS data representing an integral over the first decimeters and the simulated data derived from the mHM for three distinct soil depths, at 0–5 cm (green), 5–25 cm (purple), and 25–60 cm (brown).

### 2.4.1 Desilets based method

In the present study, we utilize the soil moisture information from the mHM to convert it into neutron counts using the empirical-based approach by Desilets et al. (2010). We also added lattice water and bulk density information following the  
 190 suggestions from Dong et al. (2014) and Hawdon et al. (2014), respectively. This empirical approach makes use of a free scaling parameter  $N_0$ , which represents the neutron count rate of a particular CRNS probe under dry soil conditions. This parameter is typically site-specific but does not change over time, as noted by Franz et al. (2013) and Hawdon et al. (2014). It is also specific to the particular CRNS detector and may be influenced by factors such as terrain (topography), local soil, vegetation characteristics, and additional hydrogen pools (e.g., from organic matter) at each observation site. Therefore, the determination

195 of  $N_0$  by local soil sampling campaigns is necessary. Once determined, , the parameter  $N_0$  should be kept constant or carefully calibrated within limits of not more than  $\pm 5\%$ . As a sensitive parameter,  $N_0$  strongly influences the accuracy of the mHM soil moisture results.

Soil moisture for three vertical mHM soil layers is used as input for both the Desilets method and the COSMIC operator. To improve comparability between measurements and modeling techniques, Schrön et al. (2017) proposed to weight the soil  
200 moisture values of each layer by their depth. This approach results in a depth-weighted average SWC,  $\theta_{avg}$  that better represents the complex behaviour of neutrons to probe the soil.

$$N_{Des} = N_{0,Des} \left( \frac{a_0}{(\theta_{avg} + \theta_{lw}) / (\rho_b / \rho_w) + a_2} + a_1 \right) \quad (1)$$

Among the four parameters,  $a_{0..2}$  were determined empirically by Desilets et al. (2010). The authors derived  $a_0 = 0.0808$ ,  $a_1 = 0.372$ , and  $a_2 = 0.115$  for  $\theta > 0.02 \text{ gg}^{-1}$ . The fourth parameter,  $N_{0,Des}$  is fixed based on field measurements, with its  
205 value taken from Bogena et al. (2021). Since neutrons are sensitive to all kinds of hydrogen in the footprint, the variable  $\theta$  denotes not only soil moisture, it is rather assumed to also include lattice water,  $\theta_{lw}$ , as well as water equivalent from soil organic carbon and vegetation biomass. More precisely,  $\theta_{lw}$  is the grid average volumetric water content of the equivalent  
lattice water content of the CRNS area ( $\text{cm}^3 \text{ cm}^{-3}$ ),  $\rho_b$  ( $\text{g cm}^{-3}$ ) is the bulk density of the dry soil, usually determined from soil samples, and  $\rho_w = 1 \text{ g cm}^{-3}$  is the density of water. Regarding the variables of Soil Organic Carbon (SOC) and biomass,  
210 it's important to note that these variables are often not readily available, especially when it comes to biomass data. For lattice water, we assume a linear relationship to clay content (Avery et al., 2016):

$$\theta_{lw} = \theta_{lw0} \cdot C + \theta_{lw1}, \quad (2)$$

$C$  denotes the clay fraction in % (Greacen, 1981). The derived quantity lattice water,  $\theta_{lw}$ , is regionalized based on  $C$  and varies between 0.0 and  $0.1 \text{ m}^3/\text{m}^3$ . In order to obtain the average soil moisture for a layered soil moisture profile within mHM,  
215 the following averaging equation is employed:

$$\theta_{avg}(w, \theta) = \frac{\sum_{i=1}^n w_i \theta_i}{\sum_{i=1}^n w_i} \quad (3)$$

where the volumetric soil water content at a specific layer of mHM in a given profile is denoted by  $\theta_i$  ( $\text{m}^3 \text{ m}^{-3}$ ). The total number of layers in all soil sampling profiles is represented by the variable  $n$ , and the weight assigned to layer  $i$  is denoted by  $w_i$ . In the uniformly weighted approach, all weights equal one:

$$220 \quad N_{Des,U} = N_{Des}(w_i = 1) \quad \forall i. \quad (4)$$

In the weighted-averaging approach, the weights are determined based on Schrön et al. (2017):

$$N_{\text{Des},w} = N_{\text{Des}}(\theta_{\text{avg}}(w, \theta)), \quad (5)$$

where  $w_i = \int_{z_{i,\min}}^{z_{i,\max}} e^{-2z/D} dz \propto e^{-2z_{i,\min}/D} - e^{-2z_{i,\max}/D}$

and  $D = \varrho_b^{-1} \left( p_0 + p_1 (p_2 + e^{-p_3 r}) \frac{p_4 + \theta}{p_5 + \theta} \right)$ . (6)

225 Here, the integral goes through each horizon from  $z_{i,\min}$  to  $z_{i,\max}$  in 1 mm steps and sums up the weight over the whole layer.  $z_i$  is the depth of the given soil moisture layer  $i$ ,  $D$  is the average vertical footprint depth of the neutrons,  $p_i$  are numerical parameters presented in Schrön et al. (2017), and  $r$  (m) represents the distance from the sensor. It should be noted that the equation for  $D$  is valid for  $\varrho_b > 1.0 \text{ g cm}^{-3}$  and soil moisture contents above  $\theta > 2 \%$  (Kasner et al., 2022). In our model, we set  $r = 1 \text{ m}$  which is sufficient to represent the average depth across the footprint radius within the model grid. The soil  
230 moisture profile is converted to a single average neutron count per grid cell using Eqs. 1–5.

#### 2.4.2 Cosmic Ray Soil Moisture Interaction Code (COSMIC)

The Cosmic Ray Soil Moisture Interaction Code (COSMIC) is an neutron forward operator that has been developed for data assimilation applications (Shuttleworth et al., 2013). The model aims at mimicing the physical processes of neutron transport in the vertical dimension of the soil using a simplified analytical formulation of the most relevant mechanisms and their effective  
235 parameterizations. Shuttleworth et al. (2013) reported that this lack of complexity might introduce systematic errors for typical soil moisture profiles on the order of 2% compared to physics-based models (e.g., Köhli et al., 2023). However, the simplified approach allows to estimate neutron counts with a computational efficiency that is several orders of magnitude faster.

The COSMIC model assumes a downwards attenuation of incoming high-energy neutrons with soil depth, the production of fast neutrons in each soil layer, and an isotropic scattering of the resulting fast neutrons that is projected upwards. These  
240 processes exhibit a parametric dependency on soil properties and water content and lead to a resulting neutron count value for each grid cell in mHM.

$$N_{\text{COSMIC}} = N_{0,\text{COSMIC}} \sum A_{\text{high}}(z) X_{\text{eff}}(z) A_{\text{fast}}(z), \quad (7)$$

where  $A_{\text{high}}(z) = e^{-\Lambda_{\text{high}}(z)}$ ,

$$A_{\text{fast}}(z) = \frac{2}{\pi} \int_0^{\pi/2} e^{-\Lambda_{\text{fast}}(z)} (\cos \varphi)^{-1} d\varphi,$$

245  $X_{\text{eff}}(z) = \alpha_{\text{COSMIC}} X_{\text{soil}} + X_{\text{water}}$ .

We used soil samples from the COSMOS-Europe paper (Bogena et al., 2022) to run the COSMIC model in order to determine the scaling factor  $N_{0,\text{COSMIC}}$ , following the established strategies (Shuttleworth et al., 2013; Patil et al., 2021; Baatz et al., 2014). In Eq. 7,  $A_{\text{high}}$  represents the high-energy neutron attenuation,  $A_{\text{fast}}$  represents the fast neutron attenuation, and  $X_{\text{eff}}$  represents

the production of fast neutrons from high-energy neutrons at any level in the soil. It takes into account the different mechanisms  
 250 in both, water and soil, where the soil is typically less effective in producing fast neutrons by a factor of  $\alpha_{\text{COSMIC}} \approx 0.24$   
 ( $\text{g cm}^3 \text{g}^{-1}$ ), depending on bulk density.

$$X_{\text{soil}}(z) = \Delta z \rho_{\text{b}}, \quad (8)$$

$$X_{\text{water}}(z) = \Delta z \rho_{\text{water}} (\theta_z + \theta_{\text{lw}}), \quad (9)$$

The effective attenuation of high-energy and fast neutrons in the soil-water composite are described by physically motivated  
 255 functional relationships with effective length scales  $L_i$ .

$$\Lambda_{\text{high}}(z) = \frac{X_{\text{soil}}(z)}{L_1} + \frac{X_{\text{water}}(z)}{L_2}, \quad (10)$$

$$\Lambda_{\text{fast}}(z) = \frac{X_{\text{soil}}(z)}{L_3} + \frac{X_{\text{water}}(z)}{L_4}. \quad (11)$$

The length constants  $L_1, L_2, L_3$ , and  $L_4$  (in  $\text{g cm}^{-2}$ ) are related to local soil properties. COSMIC uses several time-invariant,  
 site-independent, and site-specific parameters, including  $L_1 = 162.0$  ( $\text{g cm}^{-2}$ ),  $L_2 = 129.1$  ( $\text{g cm}^{-2}$ ), and  $L_4 = 3.16$  ( $\text{g cm}^{-2}$ ),  
 260 as reported by Shuttleworth et al. (2013), regardless of location. However, the  $L_3$  ( $\text{g cm}^{-2}$ ) parameter varies with soil bulk  
 density  $\rho_{\text{b}}$  which may change with depth. In mHM, this is expressed by a linear relationship of regionalized parameters  $L_{30}$   
 and  $L_{31}$ :

$$L_3 = L_{30} \rho_{\text{b}} - L_{31}. \quad (12)$$

The original formulation of the COSMIC method has been further extended by the inclusion of layer-wise lattice water content  
 265 and bulk density. Furthermore, COSMIC inside mHM has been numerically optimized to substantially increase the computa-  
 tional performance. This includes the calculation of the projected integral (Eq. 7) based on lookup tables.

## 2.5 Constraining of model parameterization

In this study, we employ a model calibration technique to identify the most suitable parameter values for the mHM. Specifically,  
 we utilize a total of 28 parameters for the Desilets based method and 30 parameters for the COSMIC method which includes  
 270 hydrologic processes related to: snow, soil moisture, and neutron counts dynamics. The process of model calibration involves  
 modifying the parameter values of the model to achieve a satisfactory standard for an objective function by comparing the  
 predicted output with the observed data (James, 1982). We use the general concept of the KGE as a weighted combination  
 of the three components (bias, variability, and correlation terms) to evaluate our simulation (Gupta et al., 2009). We excluded  
 the correlation component from (Gupta et al., 2009) equation as our simulation already exhibited satisfactory correlation due  
 275 to strong seasonality, we opted not to consider it in our assessment (objective function), as it accounted for 33% of the total  
 weighting in the overall KGE score. Seasonality is an inherent characteristic in the northern hemisphere where precipitation  
 minus evaporation is mostly driven by evapotranspiration. Even if a random parameter is selected correlation will always be  
 higher because the meteorological forcing is the precipitation - evaporation is seasonal. This modified  $\text{KGE}_{\alpha\beta}$  only depends

on variability ( $\alpha$ ) and bias ( $\beta$ ) and variants of it have been used also in other studies (see, e.g., Martinez and Gupta, 2010; Mai, 280 2023). We utilize observed neutron count data from CRNS and estimated neutron count data from the mHM to calculate various metrics such as the modified Kling-Gupta efficiency coefficient ( $KGE_{\alpha\beta}$ ), root mean square error (RMSE), and percentage bias (PBIAS) by Gupta et al. (1999). The optimal PBIAS value is 0, with lower values indicating more accurate model simulations. Positive values indicate underestimation by the model, while negative values indicate overestimation. This approach allows us to minimize uncertainty in the simulated neutron count data by comparing it to observed data and determining the optimal 285 parameter values for the mHM. A summary of the individual parameters and their ranges can be found in Supplementary Table S3.

### 3 Results

#### 3.1 Analysis of posterior parameters across the study sites

Figure. 4 shows the normalized range of posterior parameter sets of mHM, compared across the four study sites: *Grosses Bruch*, *Hohes Holz*, *Hordorf*, and *Cunnersdorf*. Out of 30 parameters, the 10 most relevant parameters for root-zone soil moisture dynamics are presented (see Table 2 for parameter description and ranges). The other parameters are shown in the supplementary material. Figure. 4 indicates that the selected parameters showed a well-constrained distribution within their allowed range across the study sites. Among them, at the *Grosses Bruch* site we find the most stable parameter distribution with low variability (small error bars) across most of the inferred parameters, including vertical root fractions of different vegetation 290 types (*rotfrcoffore*, *rotfrcofperv*). A relatively higher variability (large error bars) in the posterior parameter distributions is noticed for *ptflw0*, *ptflw1* and *ptfhigdb* – these parameters are related to the estimation of lattice water and bulk density. Pedo-transfer function (PTF) related parameters that control the saturated soil water content (*ptflowconst*, *ptflw1*, *ptflw0*) at the *Hohes Holz* site showed the lowest variability, reflecting a consistent behavior for inferring these parameters at this site. The site at *Hordorf* shows moderate variability across most of the analysed parameters especially for the *orgmatperv*, *ptfhigdb*, *ptflw1*, 300 *ptflw0*. Overall across all the study sites, the posterior distribution of parameter *ptflowdb* exhibits high variability, reflecting the importance of further constraining of this parameter. There is a varying degree of sensitivity across the parameters, but certain parameters consistently demonstrate sensitivity across the site (*rotfrcoffore*, *ptflowdb*, *ptfhigclay*, *ptflowconst*). This finding aligns with previous studies (Cuntz et al., 2015; Koch et al., 2022; Demirci and Demirel, 2023), which also identified these parameters as sensitive in mHM across various study locations.

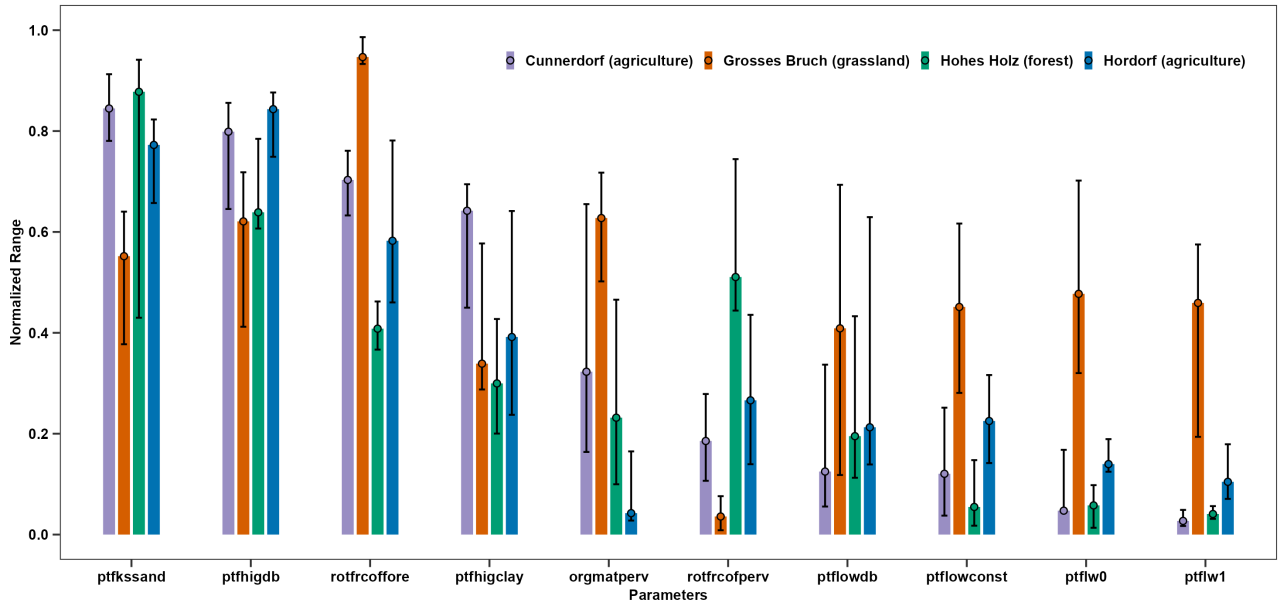


**Figure 4.** Bar plot showing posterior distribution of model parameters across three land cover types, calibrated using cosmic-ray neutron sensing data. Parameter values are scaled between 0 and 1. The whiskers represent the upper and lower limits of the inter-quantile range, while the dots represent the median values of the normalized range for each parameter.

**Table 2.** Description of ten selected parameters and their ranges in mHM.

Parameter No	Parameter Name	Description	Min	Max
$\beta_1$	rotfrcofperv	Root fraction coefficient pervious	0.001	0.09
$\beta_2$	rotfrcoffore	Root fraction coefficient forest	0.9	0.999
$\beta_3$	ptflowdb	PTF saturated water content: coefficient bulk density	-0.27	-0.25
$\beta_4$	ptflowconst	PTF saturated water content: constant	0.75	0.8
$\beta_5$	ptfkssand	PTF hydraulic conductivity: Sand	0.006	0.026
$\beta_6$	ptfhigdb	Coefficient for bulk density in pedo-transfer function for soils with sand content higher than 66.5%	-0.35	-0.3
$\beta_7$	ptfhigclay	Coefficient for clay in pedo-transfer function	-0.0012	-0.0008
$\beta_8$	orgmatperv	Organic matter content for pervious zone	0	5
$\beta_9$	ptflw1	PTF lattice water	0	0.2
$\beta_{10}$	ptflw0	PTF lattice water	0	0.05

### 305 3.2 Time series analysis of simulated neutron counts

The study conducts simulations of neutron counts in mHM using soil moisture parameterizations, with results presented in Figs. 5–6 across different land cover sites. In these figures, the grey dots represent the CRNS soil moisture measurements. The  $N_0$  parameter values, taken from field measurement, are documented for each site, including *Grosses Bruch*, *Hohes Holz*, *Hordorf*, and *Cunnerdorf*. We utilized measurement data from COSMOS Europe Bogen et al. (2022), where neutron counts were converted to soil moisture,  $\theta(N)$ , using the methodology from Desilets et al. (2010). The simulated neutron counts were based on the simulated soil moisture content at the modeled soil horizons i.e., 0–5 cm, 5–25 cm, and 25–60 cm. The results of the ensemble runs show that the precision is higher for the behavioral simulation ensembles 0.1 % (represented by dark gray shaded areas) than in the unconstrained simulated data 1 % (represented by light gray shaded areas). We select the best 0.1 % with the highest KGE from 100 000 model runs, and the results are presented in Tab. 3. However, a larger discrepancy was noted at *Hohes Holz* a dense forest site, across all three methods. This difference could be attributed to the Leaf Area Index (LAI), biomass and vegetation dynamics, which are not currently integrated into mHM. Recent efforts by Bahrami et al. (2022) aim to address vegetation dynamics in mHM, but this integration is still incomplete. Among the methods, the  $N_{\text{COSMIC}}$  method performs best at the forest site (*Hohes Holz*), whereas at the agricultural sites (*Hordorf* and *Cunnerdorf*), the  $N_{\text{Des,W}}$  method performs slightly better. In the grassland site (*Grosses Bruch*), the uniform method  $N_{\text{Des,U}}$  slightly outperforms the other two methods i.e.,  $N_{\text{Des,W}}$  and  $N_{\text{COSMIC}}$ . In general, we observe good model performance for all methods indicated by a Kling-Gupta efficiency greater than 0.75 and a percent bias (PBIAS) below  $\pm 10\%$  across the majority of investigated sites and methods. These results suggest that the neutron-forward models match the observed neutron counts well. However, the mean ensemble had difficulties reproducing the neutron counts for the *Hohes Holz* site in all three methods.

The incorporation of dynamic vegetation in models is important as it can impact the model parameter LAI, which in turn can affect root water uptake and soil water content. Currently, these factors are not considered in the models, leading to a permanent and systematic shift in these variables each year (Zink et al., 2017; Massoud et al., 2019).

The results also highlight the uncertainties associated with model simulations and the sensitivity of the objective function. We find that ten soil moisture-related parameters, mentioned in Table 2, have the most significant impact on the objective function  $\text{KGE}_{\alpha\beta}$ , compared to the other parameters of mHM. The parameter  $lw$  directly affects the neutron count simulations, while the other parameters correspond to the fractions of vegetation roots in different soil layers that directly affect the water availability related stress for the estimation of actual evapotranspiration, and thereby the soil-water dynamics (Samaniago et al., 2010b; Kumar et al., 2013b). The best parameter set values in mHM across all sites and methods are given in (Supporting Information Table S3).

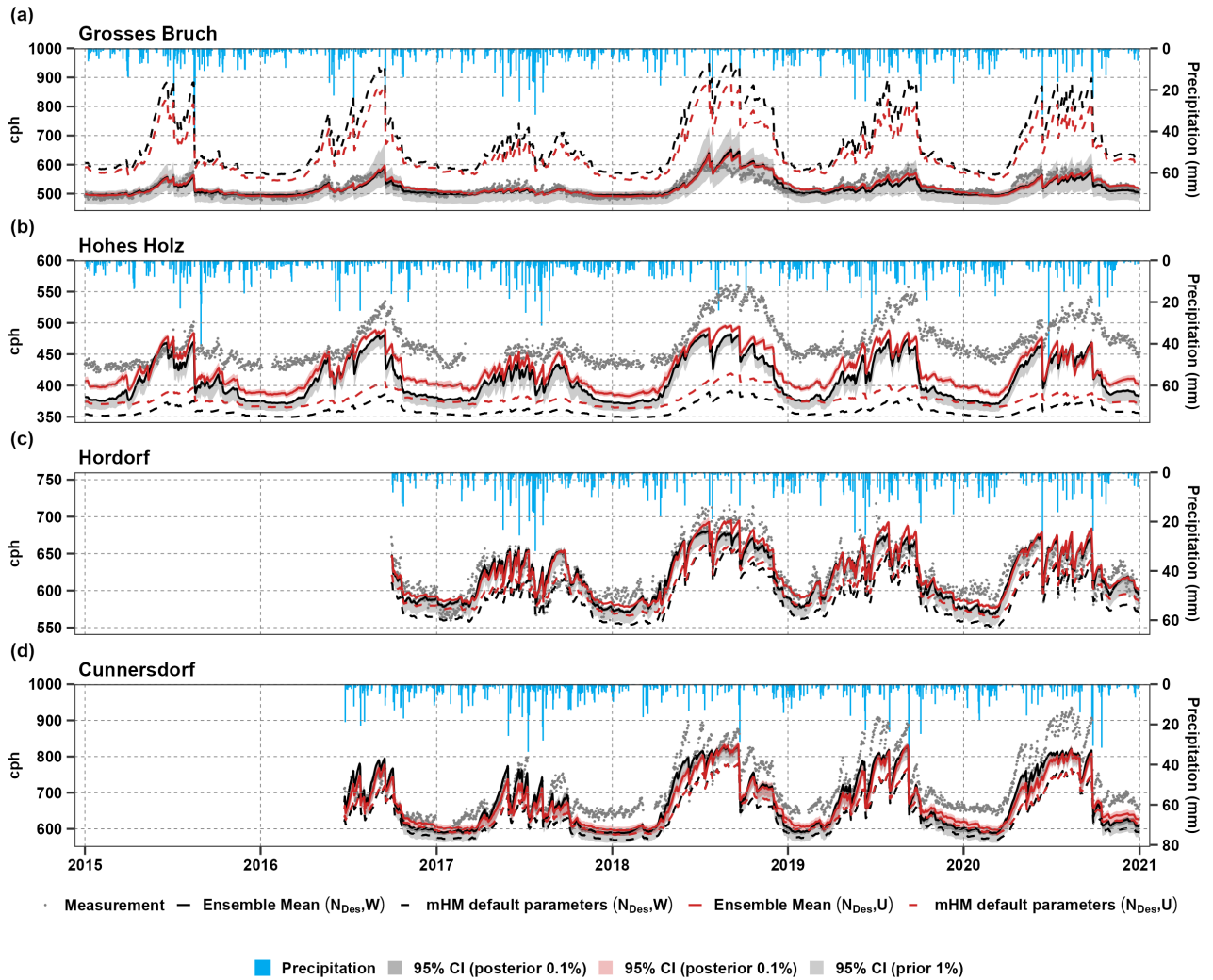


**Figure 5.** Simulated daily time series of black for  $N_{Des,W}$ , red for  $N_{Des,U}$  for the four sites. The black lines represent the median of the behavioural simulation ensembles that satisfy the objective function which is LHS10 ensemble members. The light grey shaded areas represent the 95% CI of the simulation ensembles corresponding to different levels of constraining which is LHS1000 ensemble members, and the observation is shown in grey points. Precipitation is shown in blue color on the top.



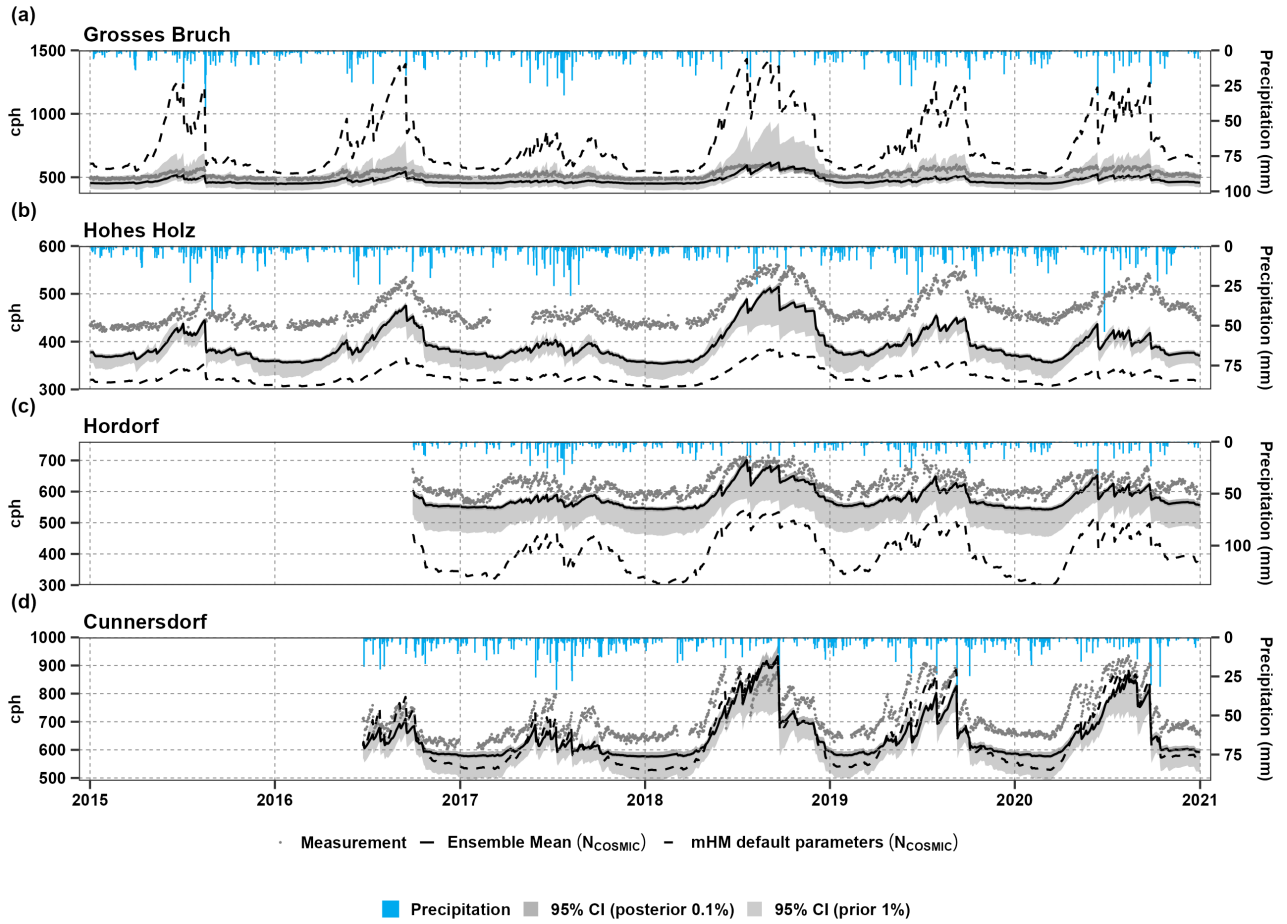


**Figure 6.** Simulated daily time series of  $N_{\text{COSMIC}}$  for the four sites. The black lines represent the median of the behavioural simulation ensembles that satisfy the objective function which is LHS10 ensemble members. The light grey shaded areas represent the 95% CI of the simulation ensembles corresponding to different levels of constraining which is LHS1000 ensemble members, and the observation is shown in grey points.

### 3.3 Model calibration statistics and evaluation

335 In addition to  $\text{KGE}_{\alpha\beta}$ , the three metrics KGE, RMSE, and PBIAS are used to evaluate further the mHM neutron counts simulated with observed CRNS data. We employ LHS to generate a parameter sample of 100 000 for the three methods, namely  $N_{\text{Des,U}}$ ,  $N_{\text{Des,W}}$  and  $N_{\text{COSMIC}}$ , by uniformly distributing the ranges provided in the (supplementary Table S2). The top 10 parameter sets are found to perform satisfactorily with a KGE range of 0.75 to 0.9, as demonstrated in Table 3. The calibrated parameter sets obtained from different objective functions are also evaluated and compared using various statistical

340 indices, as shown in Figure 7. The results for the COSMIC method indicate that the main contribution to poorer results during the evaluation period was due to the variability term ( $\alpha$ ). The boxplot displayed in Figure 7 illustrates the threshold achieved by

the top 1000, 100, and 10 LHS members, along with the corresponding percentage of the best 10 LHS parameter sets that meet the threshold. Among the 30 parameters selected to simulate neutron counts, this plot provides an overview of the distribution of results and their variability with respect to the threshold criteria.

**Table 3.** Performance metrics for model calibration (2014-2021) using various methods: Kling-Gupta Efficiency (KGE), Root Mean Square Error (RMSE), and percentage bias (PBIAS) across different sites. The observed neutron counts were compared with the simulated neutron counts from the mHM.

Sites	<i>Grosses Bruch</i>			<i>Hohes Holz</i>			<i>Hordorf</i>			<i>Cunnersdorf</i>		
Methods:	$N_{Des,U}$	$N_{Des,W}$	$N_{COSMIC}$	$N_{Des,U}$	$N_{Des,W}$	$N_{COSMIC}$	$N_{Des,U}$	$N_{Des,W}$	$N_{COSMIC}$	$N_{Des,U}$	$N_{Des,W}$	$N_{COSMIC}$
<b>mHM default run</b>												
KGE	-0.74	-1.46	-5.52	0.33	0.26	0.44	0.73	0.81	-0.06	0.63	0.71	0.64
RMSE	133.78	175.1	309.8	89.61	108.15	139.5	27.46	36.31	223	80.41	90.18	85.5
PBIAS	23.3%	30.2%	46%	-18.6%	-22.6%	-29.6%	-3.5%	-5.2%	-35.2%	-9.8%	-11.6%	-10%
<b>mHM calibrated</b>												
KGE	0.85	0.83	0.78	0.77	0.75	0.79	0.87	0.86	0.84	0.81	0.90	0.85
RMSE	16.12	17.84	50.55	45.42	59.9	73.5	16.83	17.89	48	54	51.83	81
PBIAS	0%	-0.7%	-9%	-8.7%	-12%	-15.4%	-0.1%	-0.6%	-15.4%	-6.2%	-5.7%	-9.9%

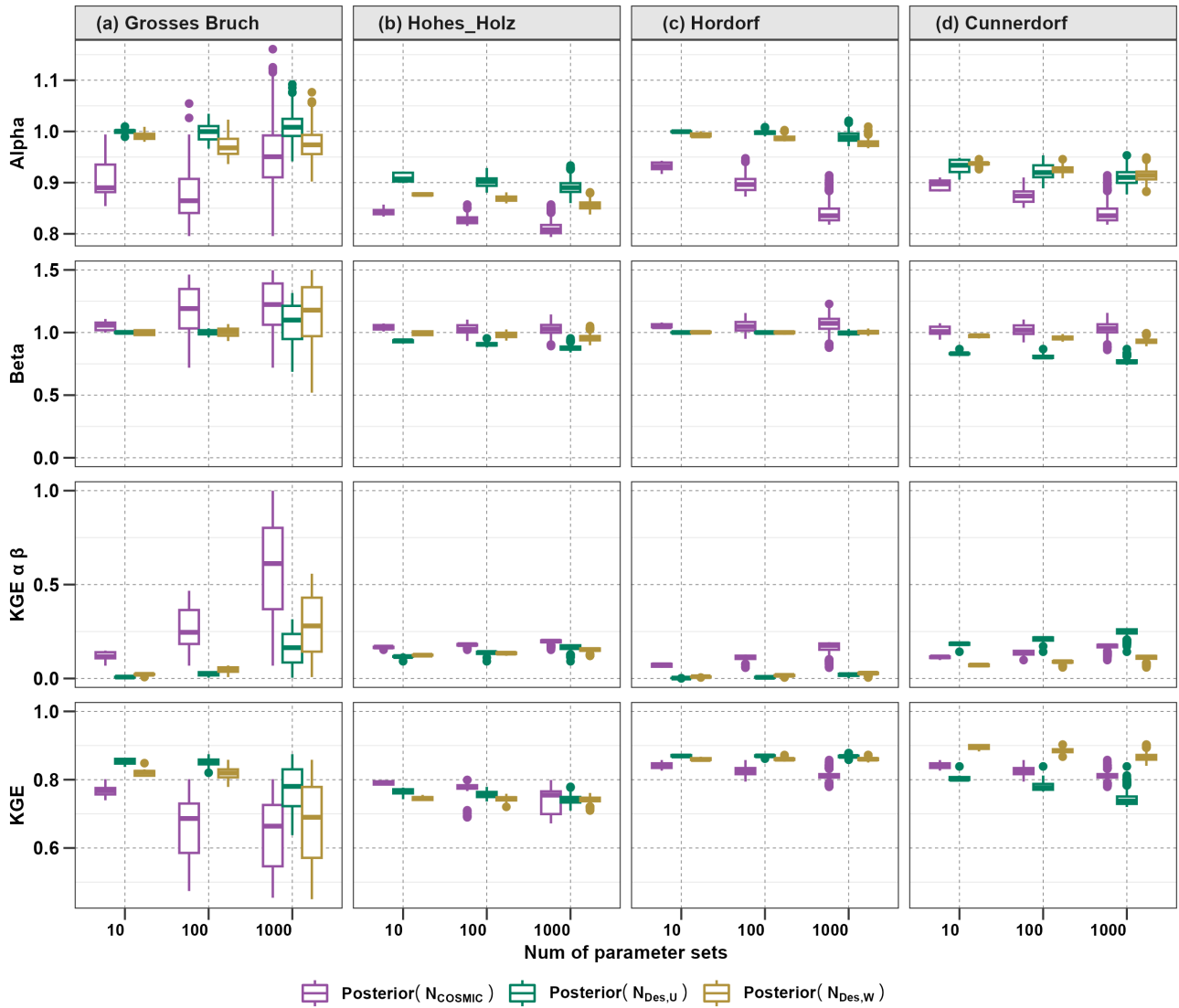


**Figure 7.** Evaluation of model performance using boxplots constraining of 1000 to the best 10 parameters set at four different sites, using three different methods, namely  $N_{\text{Des,W}}$  in brown,  $N_{\text{Des,U}}$  in green, and  $N_{\text{COSMIC}}$  in purple. The figure presents four subplots, where (a) represents Alpha, (b) Beta, (c)  $\text{KGE}_{\alpha\beta}$ , and (d) Kling-Gupta efficiency (KGE) and its components, i.e., the variability term (perfect value: 1), and bias term (perfect value: 1), respectively.

### 345 3.4 Comparing evapotranspiration at Hohes-Holz: eddy covariance observed data vs mHM simulation

The ensemble model of (10 members) simulations are further validated with evapotranspiration (ETA) data to assess the model's ability to represent other fluxes and states in addition to neutron counts. This validation uses ETA observational data from eddy covariance measurements provided by the Integrated Carbon Observation System (ICOS) at *Hohes Holz* (Warm Winter, 2022).

In terms of temporal dynamics, the model is capable to capture the observed ETa quite well at the study site, as shown in Figure 8. Panel (c) displays the scatter plot incorporating linear regression models to quantify the relationships between observed and mHM-simulated ETa during both the growing and non-growing seasons. This plot provides insights into the seasonal variations in the relationship between observed and simulated ETa. It suggests that the model performs best during winter, while its performance during summer is comparatively weaker. The correlation coefficients ( $r$  values) for each season are as follows: autumn [SON] ( $r = 0.72$ ), spring [MAM] ( $r = 0.75$ ), summer [JJA] ( $r = 0.35$ ), and winter [DJF] ( $r = 0.85$ ). It is worth noting that winter shows the highest correlation between observed and simulated ETa, while summer exhibits the lowest correlation. The most significant deviation in terms of RMSE is evident during the summer, when ETa is highest, while the smallest difference is in winter when ETa has less impact. The model slightly overestimates ETa in summer and spring, possibly because of the absence of a dynamic vegetation growth module in the mHM, also discussed for evapotranspiration by Zink et al. (2017). The temporal dynamics of the model-simulated evapotranspiration are in good agreement with the observed data from the *Hohes Holz* forest eddy covariance site, taken from Warm Winter (2022), as illustrated in Figure 8a. Daily correlation between observed and simulated evapotranspiration is observed high in the growing season at  $r = 0.8$ , whereas the lowest correlation is found in the non-growing season at  $r = 0.53$  in Figure 8c. The highest deviation in terms of RMSE is observed during summer when the highest fluxes occur, and the lowest during winter, in which the contribution of ETa is lowest.

In Figure 8b, the prior and posterior parameter distributions of evapotranspiration for *Hohes Holz* are displayed. The prior distribution represents the 100 000 parameters set utilized for the neutron counts simulation under Latin Hypercube Sampling (LHS). The results demonstrate that the ensemble model of 10-member simulations (posterior) for neutron counts can also effectively capture evapotranspiration, exhibiting a root mean square error (RMSE) of  $0.76 \text{ mmd}^{-1}$  of the growing season and  $0.25 \text{ mmd}^{-1}$  for non-growing when compared to observed ICOS data and simulated mHM. When compared to the model simulations with prior parameter sets, we notice a substantial improvement in ET simulations (mean RMSE of  $0.85 \text{ mmd}^{-1}$  to  $0.76 \text{ mmd}^{-1}$ ). Furthermore, the RMSE range is also narrower for the posterior simulations compared to the prior ones which further demonstrated the additional value of incorporating CRNS measurements in improving the consistency of both modeled soil moisture and evapotranspiration estimates. Nevertheless, the overall agreement between modeled and observed ETa is reasonably good; and the analysis reveals further improvement of model performance in the growing season.

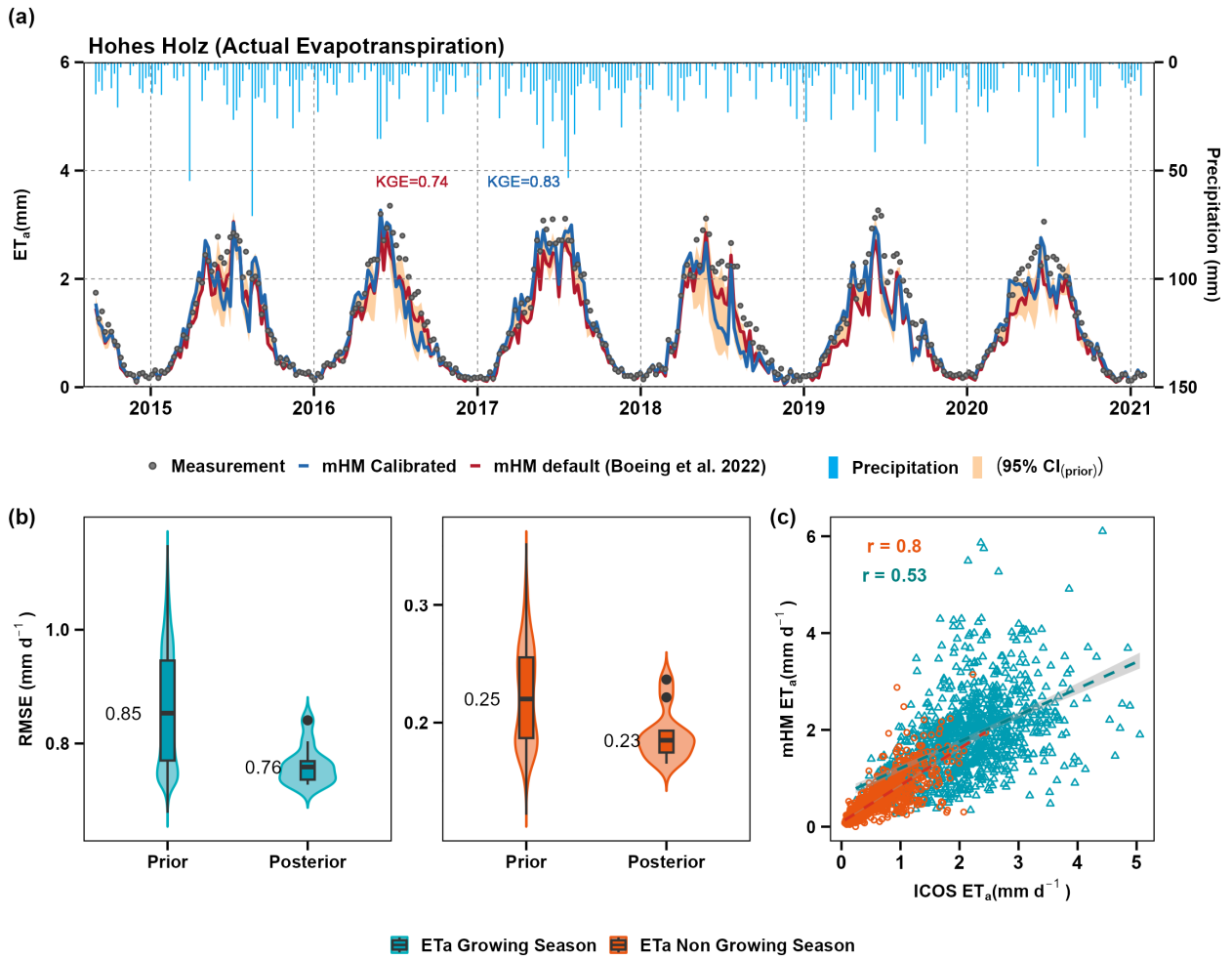


**Figure 8.** (a) Comparison of weekly observed actual evapotranspiration (grey dots) and simulated actual evapotranspiration using the default mHM parameters by Boeing et al. (2022) (red line), the calibrated simulation (blue dots), and the prior range of 100 000 realizations in (orange) color over the *Hohes Holz* site. (b) Boxplot of daily actual evapotranspiration (ET<sub>a</sub>) differences between the growing and non-growing seasons, comparing two selected prior with 100 000 simulations, the values represent the mean of the statistical metrics and posterior with 10 ensemble member distributions using the root mean square error (RMSE) as the evaluation metric ( $\mu\text{gm}^3$ ). (c) scatterplots of modeled vs. observed ET on a daily basis from ICOS during the growing season from March to August (green) and non-growing season from September to February (brown) at *Hohes Holz* eddy covariance station in a forest.

## 4 Discussion

375 This study assessed the suitability of CRNS observations at four sites to enhance soil moisture representation in mHM. The theoretical measurement depth for the cosmic-ray probe varies, ranging from  $\sim 12$  cm in wet soils to  $\sim 76$  cm in dry soils (Zreda et al. (2008, 2012a); Rosolem et al. (2014)).

To improve the soil moisture profile representation within mHM it is a major challenge to use a single vertically integrated CRNS measurement. In order to have a fair comparison between the model and observed CRNS data, two conceptually different approaches were integrated into mHM to calculate neutron counts from different SWC horizon depths i.e., an empirical method based on Desilets et al. (2010), and neutron forward operator (COSMIC) based on Shuttleworth et al. (2013). Since the empirical method is described by an analytical expression, taking into account the uniform average of the soil moisture layers, it is straightforward to implement and therefore most commonly used (Zreda et al., 2012b; Rivera Villarreyes et al., 2011; Andreasen et al., 2017; Bogen et al., 2022). However, the method comes with the risk of missing a representation of the vertical profile of soil properties and water content. Therefore, we extended this uniform-averaging scheme with a vertical weighting scheme to mimic the sensitivity of the neutrons to the upper layers both weighted and non-weighted soil moisture approaches in the context of CRNS have been discussed (Rivera Villarreyes et al., 2014; Baroni and Oswald, 2015; Schreiner-McGraw et al., 2016; Zreda, 2016; Schrön et al., 2017; Vather et al., 2019; Barbosa et al., 2021). The COSMIC operator also accounts for the full soil moisture profile, following the track and attenuation of the neutrons in and out of the soil column. The mHM is now able to simulate neutrons directly with all three approaches. The presented results confirmed general consistency with CRNS observations at four sites in Germany (Figs. 5 and 6).

Agricultural land presents a valuable opportunity to examine the interaction between soil moisture dynamics, crop growth, irrigation methods, and vegetation dynamics. *Hordorf* and *Cunnerdorf* are specific agricultural sites where seasonal changes in aboveground biomass are expected to be larger due to crop growth and harvest compared to grassland and forest sites. The study by Schrön et al. (2017) found that the revised weighting strategy for CRNS data improved the accuracy of soil moisture predictions at agriculture sites, but there is still room for improvement in capturing local dynamics through revised parameters in the CRNS model. Our results also showed that at the agriculture site, the  $N_{\text{Des,U}}$  methods in mHM slightly out-performed the other methods.

We also investigated *Hohes Holz*, a forest site, and observed an early simulation of approximately 28 days in the simulation of neutron counts compared to the observations. The early simulation phase could be attributed to the limitation of mHM in simulating the dynamics of detailed vegetation mechanisms Zink et al. (2017). While CRNS and TDR generally agree at this site, the discrepancy shown in our results could be attributed to issues related to process representation in mHM Boeing et al. (2022). Simulation of neutron data within the mHM and subsequently comparing it with observed counts can enhance the accuracy and precision of soil moisture measurements. Future research can focus on exploring the potential relationships between CRNS data and soil moisture anomalies, thus furthering our understanding of the dynamics of drought and assisting in the development of efficient drought monitoring and mitigation strategies.

To cross-evaluate our results, we generated and filtered the 100 000 regionalized parameter sets based on observed neutron counts for behavioral solutions. After selecting the most effective solutions, we conduct cross-validation by comparing the mHM simulations of evapotranspiration against observational data from eddy covariance measurements ICOS (Warm Winter, 2022; Pohl et al., 2023) at the *Hohes Holz*. Figure 8 shows the scatter including the seasonal correlation coefficient at the forest site. The results indicate low correlations in summer, likely due to mHM’s limitations in capturing evapotranspiration values with mHM’s static vegetation module. However, the model performs well in winter, with a high correlation between observed and simulated values of evapotranspiration, the results confirm the findings from Zink et al. (2017), who used mHM to estimate evapotranspiration, groundwater recharge, soil moisture, and runoff with 4 km spatial and daily temporal resolutions (1951–2010). They utilized soil moisture observations from eddy covariance stations employing Time-Domain Reflectometer (TDR) or Frequency-Domain Reflectometer (FDR) sensors. Due to disparities in spatial representativeness and sampling depth, a direct comparison between observed and simulated soil moisture was not feasible, their findings revealed deviations in evapotranspiration during spring and in cropland areas, while soil moisture estimations exhibited good agreement with observed dynamics. The study highlights the importance of considering seasonal variations when analyzing the results. Discrepancies, such as low correlations in summer, indicate the need for improvements in capturing evapotranspiration dynamics under varying environmental conditions. Refining vegetation dynamics representation could enhance the simulation of evapotranspiration processes. Additionally, the agreement between mHM and observed soil moisture dynamics suggests variable model performance for different hydrological variables, emphasizing the need for a comprehensive assessment of its capabilities across various environmental conditions and spatiotemporal scales. The accuracy of modeled evapotranspiration is linked to soil parameterization because soil water is the main source of evaporative water. During the growing season (summer), the model exhibited the largest variability in modeled ETa (Figure 8c). This can be associated among other things with a lack of a dynamic vegetation growth module in mHM, which may not capture the onset of the vegetation period adequately. This variability could also be attributed to seasonal changes in vapor pressure difference (VPD) or more localized processes occurring at the forest site (e.g., vegetation dynamics), which are currently not considered in the model.

The *Grosses Bruch* site stands out as a mesophilic grassland site with a nearby water channel, shallow ground water, regular cattle grazing, and seasonal flooding (Hermanns et al., 2021). We find the uniformly weighted approach  $N_{Des,U}$  shows a slightly better performance than the other two methods  $N_{Des,W}$  and  $N_{COSMIC}$  (see Table. 3). The behaviour may result in a missing representation of locally significant hydrological components, such as dynamic biomass, snow, shallow ground water, or nearby surface ponding (Schrön et al., 2017). Döpfer et al. (2022) mentioned high impact of grazing on the plant traits and soil properties at this site. Additionally, the use of one grid cell measurements by mHM in our study may have limited the accuracy of our results, as the depth of measurement may not be representative of the entire soil profile. Notably, neutron counts were found to provide a more accurate representation of soil water content during June, July, August, and September, when levels tend to be lower. Further exploration of neutron counts may yield additional improvements to model performance.

Overall, the three methods ( $N_{Des,U}$ ,  $N_{Des,W}$ , and  $N_{COSMIC}$ ) in mHM were able to consistently simulate the neutron count variability throughout the available data period, with the exception of the Hohes Holz site. However, a broader confidence interval is observed, indicating a greater range of variations, which implies a higher degree of uncertainty in the  $N_{COSMIC}$ . The

COSMIC approach is more complex than the Desilets approach and as such depends on more detailed additional information about the soil properties, vegetation interception, layering, etc. If the model input data is not known in such a detail, we would expect the COSMIC model to provide more uncertain results. Moreover, all three approaches are rough approximations of the actual physical processes of neutron transport which could contribute to systematic biases of around 2 % compared to exact physics-based models (Shuttleworth et al., 2013). The simulated time series tended to slightly underestimate the CRNS neutron count rate, particularly during the dry season. This effect could be explained by the known limitations of the equations under very dry conditions, while recent approaches exist (Köhli et al., 2021) that could lead to further improvement in future studies. Nevertheless, the results generally confirmed the slightly better performance of the weighted approach  $N_{Des,W}$ , compared to the uniform  $N_{Des,U}$ , because of its more realistic representation of neutron propagation with depth. After optimizing the soil hydraulic properties based on CRNS data, the integrated signal was reproduced very well (Fig. 5). Previous studies, such as McJannet et al. (2014) or Baatz et al. (2014), have noted low experimental performance for the Universal Calibration Function (UCF) method described by Franz et al. (2013). However, we have selected the Desilets method, known as the  $N_0$  method, and the COSMIC method for specific reasons. Both methods require information from soil profiles, which is readily available in the mHM. In contrast, the Universal Transport Solution (UTS) function couples soil moisture with air humidity in a non-separable way, while no atmospheric information about air humidity is available in the distributed hydrological model mHM. The same holds for the UCF function, which additionally requires a number of parameters related to hydrogen pools not represented by mHM. In using the CRNS soil moisture measurement the drier locations show larger deviations than the wetter locations (Iwema et al., 2015). The possibility of using simulated high-resolution soil moisture profiles instead of a few measurements at different soil depths could further increase the accuracy of the model predictions (Brunetti et al., 2019).

Previous studies by Smith et al. (2019) and Liu et al. (2022) address the challenges of using the original KGE in Markov chain Monte Carlo (MCMC) methods, offering insights for accurate parameter estimation and posterior distribution exploration. To address this issue, it is recommended to use adaptations to the LHS method instead of directly using the original KGE to improve the exploration of the posterior distributions. Our approach can estimate the posterior distributions of model parameters based on the objective function  $KGE_{\alpha\beta}$  by taking the variance and bias. We compared soil moisture before and after calibrating neutron counts in mHM at four sites shown in (Fig. 9). The left panel shows the mHM's default simulation using the default parameter set from Boeing et al. (2022), whereas the right panel shows the calibrated simulation based on  $N_{Des,U}$  method. The presented depicts the CRNS soil moisture measurements (grey dots) versus the soil moisture derived from mHM in different depths (colors). Table 4 shows the corresponding performance measures. It is important to acknowledge that the optimization on observed neutron counts not only improved the soil moisture representation in mHM. At the same time, it also improved the simulated evapotranspiration, as shown in the example of Hohes Holz (compare Fig. 8a). The KGE value between modeled and measured ETa by eddy covariance observations improved significantly from 0.74 to 0.83. This provides evidence that CRNS data has the potential to improve hydrological process understanding as a whole.



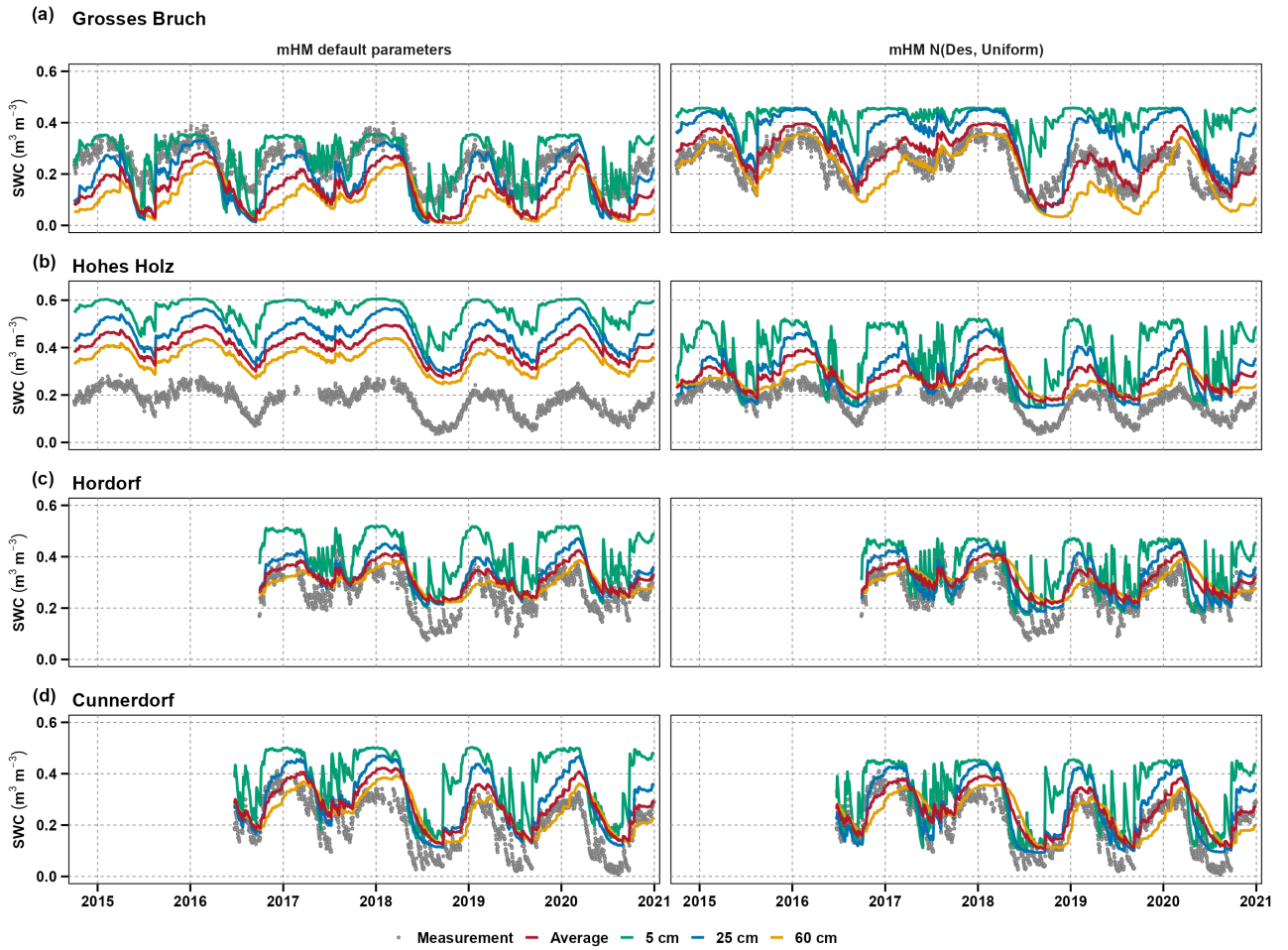


**Figure 9.** Comparison of soil water content (SWC) time series from (2015 - 2021) across all sites. The left panel illustrates the default simulation from mHM using parameters from Boeing et al. (2022), while the right panel presents the calibrated simulation based on the  $N_{Des,U}$  method. Both panels compare CRNS-derived soil moisture data (grey dots) with simulated values from mHM. The best 10 calibrated mean SWC values across different soil layers are shown, with the total average soil moisture represented by the red line.

**Table 4.** Performance metrics (KGE, RMSE, and PBIAS) for soil moisture simulations across four sites from (2014 - 2021) between  $\theta_{CRNS}$  against simulated data from mHM : *Grosses Bruch*, *Hohes Holz*, *Hordorf*, and *Cunnersdorf*. The results are compared between the default mHM run and three calibration methods ( $N_{Des,U}$ ,  $N_{Des,W}$ , and  $N_{COSMIC}$ ).

Sites	<i>Grosses Bruch</i>				<i>Hohes Holz</i>				<i>Hordorf</i>				<i>Cunnersdorf</i>			
	Default run	$N_{Des,U}$	$N_{Des,W}$	$N_{COSMIC}$	Default run	$N_{Des,U}$	$N_{Des,W}$	$N_{COSMIC}$	Default run	$N_{Des,U}$	$N_{Des,W}$	$N_{COSMIC}$	Default run	$N_{Des,U}$	$N_{Des,W}$	$N_{COSMIC}$
KGE	0.53	0.66	0.74	0.65	-0.32	0.42	0.09	0.18	0.55	0.59	0.47	0.47	0.55	0.64	0.48	0.43
RMSE	0.11	0.06	0.05	0.08	0.23	0.1	0.23	0.14	0.07	0.07	0.1	0.1	0.09	0.08	0.09	0.11
PBIAS	-44.3%	14.6%	11.5%	26.9%	131%	55%	90%	80.9%	22.4%	19%	33.8%	35%	37.6%	26.2%	39.4%	49.3%

## 5 Conclusion and future outlook

475 This study evaluates the potential of cosmic-ray neutron observations to improve soil moisture and model parameters in the mesoscale hydrological model mHM at the  $1.2 \text{ km} \times 1.2 \text{ km}$  scale across different land cover sites for the period 2014–2021. For this, we derived the neutron counts from simulated soil moisture profiles directly in the model using three different approaches: two based on an empirical function with uniform and non-uniform weighting of soil horizons, and one more complex approach based on the neutron forward operator COSMIC. Then, observed neutron counts from four sites in Germany were used to  
480 calibrate the mHM parameters. Based on the  $\text{KGE}_{\alpha\beta}$  between simulated and observed neutrons, the best 1 % parameter sets out of 100 000 model realizations were used to investigate the impact on the posterior parameter distribution and on the simulated neutrons, soil moisture, and evapotranspiration.

The evaluation of neutron counts yielded KGE values  $> 0.75$  at all four sites, indicating a satisfactory representation of the neutron counts in the model compared to the observations for the best 1 % ensemble parameter sets. The performance of the  
485 neutron counting methods varied across different land cover types. The non-uniform  $N_{\text{Des,W}}$  method generally showed good performance, particularly at the agricultural sites. While the  $N_{\text{COSMIC}}$  method performs slightly better at the forest site. The uniform  $N_{\text{Des,U}}$  method showed slightly better results at the grassland site.

There is still room for improvement in the model representation of complex sites, e.g. to better address the special site-specific conditions of the forest or grassland site, especially when using the COSMIC method. On the one hand, it is a method  
490 that aims at mimicing the physical processes of neutron transport in the soil in detailed way, but on the other hand, it relies on the detailed representation of the site characteristics in the hydrological model. This complexity could introduce additional uncertainties and limitations in the model, potentially affecting its performance, especially when the actual site is more complex than it has been modeled. The study suggests that the observed discrepancies between model and observations may be attributed to the representation of dynamic biomass, snow, surface ponding, and shallow groundwater dynamics, which are present at the  
495 grassland site, for instance. Addressing these features could further enhance the model's accuracy.

The calibration on neutron counts not only improved the soil moisture estimation but also improved the simulation of evapotranspiration at the *Hohes Holz* station. The evaluation with evapotranspiration data from eddy covariance observations indicated some deficiencies in mHM to deal with forest systems, but also great potential for CRNS measurements to improve the water partitioning in the model as a whole. In the growing season (March–August), deviations of the modeled and observed  
500 ETa indicate room for better representation of mixed soils and dynamic vegetation modules at the local scale within mHM.

In conclusion, the incorporation of neutron counts estimation into mHM by accounting for vertical soil moisture profiles improves the model's accuracy and provides a more realistic representation of soil moisture dynamics at all four study sites and even evapotranspiration at the *Hohes Holz* site. This research presents a direction for future studies to explore. Next steps could be the evaluation of neutrons and soil moisture in mHM by a large-scale soil moisture monitoring initiative, e.g.  
505 by utilizing more stationary CRNS networks (e.g., Heistermann et al., 2021; Bogena et al., 2022) or large-scale mobile CRNS campaigns (McJannet et al., 2017; Altdorff et al., 2023). To further increase accuracy and general understanding of hydrological processes, we recommend integrating both CRNS and satellite remote sensing data into mHM (e.g., based on recent insights

from Schmidt et al., 2024; Zheng et al., 2024; Rakovec et al., 2016b). Improving the model predictions will contribute to reducing the uncertainties associated with drought and flood management strategies and informed agricultural decisions.

510 *Code availability.* Simulation data is attached as supplemental material. The mesoscale Hydrological Model mHM (version 5.12) is open-source and can be freely accessed from GitLab: [https://git.ufz.de/mhm/mhm/-/tree/v5.12.0?ref\\_type=tags](https://git.ufz.de/mhm/mhm/-/tree/v5.12.0?ref_type=tags).

*Data availability.* We kindly acknowledge the German Weather Service (DWD) for providing the meteorological datasets. The terrain elevation data was collected from USGS EROS Archive - Digital Elevation - Global Multi-resolution Terrain Elevation Data 2010 (GMTED2010), available at <https://www.usgs.gov/centers/eros/science/usgs-eros-archive-digital-elevation-global-multi-resolution-terrain-elevation>. Grid-  
515 ded soil characteristics are based on the BUEK200 database obtained from the German Federal Institute for Geosciences and Natural Resources (BGR, see online at <https://geoportal.bgr.de/mapapps/resources/apps/geoportal/index.html?lang=en#/datasets/portal/154997F4-3C14-4A53-B217-8A7C7509E05F>). The geological dataset was downloaded from Institute for Biogeochemistry and Marine Chemistry, KlimaCampus, Universitt Hamburg (<https://www.geo.uni-hamburg.de/en/geologie/forschung/aquatische-geochemie/glim.html>). Leaf Area Index (LAI) dataset was downloaded from the Global Land Cover Facility (GLCF), available at <http://iridl.ldeo.columbia.edu/SOURCES/UMD/GLCF/GIMMS/NDVIg/global/index.html>. The land cover dataset was downloaded from the European Space Agency (ESA), available at [http://due.esrin.esa.int/page\\_globcover.php](http://due.esrin.esa.int/page_globcover.php). The ET data were obtained from <https://zenodo.org/record/7561854>.  
520

*Competing interests.* RK and LS are members of the editorial board of Hydrology and Earth System Sciences.

*Acknowledgements.* The authors thank all the site owners for maintaining the local sensors, particularly to F. Böttcher (DWD) and E. Thiel (SKWP). The study has been made possible by the Terrestrial Environmental Observatories (TERENO), an infrastructural fund of the  
525 Helmholtz Association. The High-Performance Computing Cluster EVE has contributed to the computation of the scientific findings. Eshrat Fatima is grateful for the financial support of the German Academic Exchange Service (DAAD) through the Graduate School Scholarship Program under Reference Number 91788160.

## References

- Albergel, C., Calvet, J.-C., Rosnay, P. d., Balsamo, G., Wagner, W., Hasenauer, S., Naeimi, V., Martin, E., Bazile, E., Bouyssel, F., et al.:  
530 Cross-evaluation of modelled and remotely sensed surface soil moisture with in situ data in southwestern France, *Hydrology and Earth System Sciences*, 14, 2177–2191, 2010.
- Aldorff, D., Oswald, S. E., Zacharias, S., Zengerle, C., Dietrich, P., Mollenhauer, H., Attinger, S., and Schrön, M.: Toward Large-Scale Soil Moisture Monitoring Using Rail-Based Cosmic Ray Neutron Sensing, *Water Resources Research*, 59, e2022WR033 514, 2023.
- Andreasen, M., Jensen, K. H., Desilets, D., Franz, T. E., Zreda, M., Boga, H. R., and Looms, M. C.: Status and perspectives on the  
535 cosmic-ray neutron method for soil moisture estimation and other environmental science applications, *Vadose Zone Journal*, 16, 1–11, 2017.
- Avery, W. A., Finkenbiner, C., Franz, T. E., Wang, T., Nguy-Robertson, A. L., Suyker, A., Arkebauer, T., and Muñoz Arriola, F.: Incorporation of globally available datasets into the roving cosmic-ray neutron probe method for estimating field-scale soil water content, *Hydrology and Earth System Sciences*, 20, 3859–3872, <https://doi.org/10.5194/hess-20-3859-2016>, 2016.
- 540 Baatz, R., Boga, H., Franssen, H.-J. H., Huisman, J., Qu, W., Montzka, C., and Vereecken, H.: Calibration of a catchment scale cosmic-ray probe network: A comparison of three parameterization methods, *Journal of Hydrology*, 516, 231–244, 2014.
- Baatz, R., Hendricks Franssen, H.-J., Han, X., Hoar, T., Boga, H. R., and Vereecken, H.: Evaluation of a cosmic-ray neutron sensor network for improved land surface model prediction, *Hydrology and Earth System Sciences*, 21, 2509–2530, 2017.
- Bahrami, B., Hildebrandt, A., Thober, S., Rebmann, C., Fischer, R., Samaniego, L., Rakovec, O., and Kumar, R.: Developing a parsimonious  
545 canopy model (PCM v1. 0) to predict forest gross primary productivity and leaf area index of deciduous broad-leaved forest, *Geoscientific Model Development*, 15, 6957–6984, 2022.
- Barbosa, L. R., Coelho, V. H. R., Scheiffle, L. M., Baroni, G., Ramos Filho, G. M., Montenegro, S. M., Almeida, C. d. N., and Oswald, S. E.: Dynamic groundwater recharge simulations based on cosmic-ray neutron sensing in a tropical wet experimental basin, *Vadose Zone Journal*, 20, e20 145, 2021.
- 550 Baroni, G. and Oswald, S.: A scaling approach for the assessment of biomass changes and rainfall interception using cosmic-ray neutron sensing, *Journal of Hydrology*, 525, 264–276, 2015.
- Beck, H. E., Pan, M., Miralles, D. G., Reichle, R. H., Dorigo, W. A., Hahn, S., Sheffield, J., Karthikeyan, L., Balsamo, G., Parinussa, R. M., et al.: Evaluation of 18 satellite-and model-based soil moisture products using in situ measurements from 826 sensors, *Hydrology and Earth System Sciences*, 25, 17–40, 2021.
- 555 BGR: Digital soil map of Germany 1 : 200,000 (BUEK 200) v0.5, [https://www.bgr.bund.de/DE/Themen/Boden/Informationsgrundlagen/Bodenkundliche\\_Karten\\_Datenbanken/BUEK200/buek200\\_node.html](https://www.bgr.bund.de/DE/Themen/Boden/Informationsgrundlagen/Bodenkundliche_Karten_Datenbanken/BUEK200/buek200_node.html), [Accessed: October 7, 2022], 2020.
- Boeing, F., Rakovec, O., Kumar, R., Samaniego, L., Schrön, M., Hildebrandt, A., Rebmann, C., Thober, S., Müller, S., Zacharias, S., Boga, H., Schneider, K., Kiese, R., Attinger, S., and Marx, A.: High-resolution drought simulations and comparison to soil moisture observations in Germany, *Hydrology and Earth System Sciences*, 26, 5137–5161, <https://doi.org/10.5194/hess-26-5137-2022>, 2022.
- 560 Boga, H., Huisman, J., Baatz, R., Hendricks Franssen, H.-J., and Vereecken, H.: Accuracy of the cosmic-ray soil water content probe in humid forest ecosystems: The worst case scenario, *Water Resources Research*, 49, 5778–5791, 2013.
- Boga, H., Schrön, M., Jakobi, J., Ney, P., Zacharias, S., Andreasen, M., Baatz, R., Boorman, D., Duygu, B. M., Eguibar-Galán, M. A., et al.: COSMOS-Europe: a European network of cosmic-ray neutron soil moisture sensors, *Earth System Science Data Discussions*, 2021, 1–33, 2021.

- 565 Bogena, H. R., Schrön, M., Jakobi, J., Ney, P., Zacharias, S., Andreasen, M., Baatz, R., Boorman, D., Duygu, M. B., Eguibar-Galán, M. A., et al.: COSMOS-Europe: a European network of cosmic-ray neutron soil moisture sensors, *Earth System Science Data*, 14, 1125–1151, 2022.
- Brunetti, G., Bogena, H., Baatz, R., Huisman, J. A., Dahlke, H., and Vereecken, H.: On the information content of cosmic-ray neutron data in the inverse estimation of soil hydraulic properties, *Vadose Zone Journal*, 18, 1–24, 2019.
- 570 Chan, S. K., Bindlish, R., O’Neill, P., Jackson, T., Njoku, E., Dunbar, S., Chaubell, J., Piepmeier, J., Yueh, S., Entekhabi, D., et al.: Development and assessment of the SMAP enhanced passive soil moisture product, *Remote sensing of environment*, 204, 931–941, 2018.
- Chen, F., Crow, W. T., Starks, P. J., and Moriasi, D. N.: Improving hydrologic predictions of a catchment model via assimilation of surface soil moisture, *Advances in Water Resources*, 34, 526–536, 2011.
- Cuntz, M., Mai, J., Zink, M., Thober, S., Kumar, R., Schäfer, D., Schrön, M., Craven, J., Rakovec, O., Spieler, D., et al.: Computationally  
575 inexpensive identification of noninformative model parameters by sequential screening, *Water Resources Research*, 51, 6417–6441, 2015.
- Demirci, U. and Demirel, M. C.: Effect of Dynamic PET Scaling with LAI and Aspect on the Spatial Performance of a Distributed Hydrologic Model, *Agronomy*, 13, 534, 2023.
- Desilets, D., Zreda, M., and Ferré, T. P.: Nature’s neutron probe: Land surface hydrology at an elusive scale with cosmic rays, *Water Resources Research*, 46, 2010.
- 580 Dimitrova-Petrova, K., Geris, J., Wilkinson, M. E., Rosolem, R., Verrot, L., Lilly, A., and Soulsby, C.: Opportunities and challenges in using catchment-scale storage estimates from cosmic ray neutron sensors for rainfall-runoff modelling, *Journal of Hydrology*, 586, 124–137, 2020.
- Dong, J. and Ochsner, T. E.: Soil texture often exerts a stronger influence than precipitation on mesoscale soil moisture patterns, *Water Resources Research*, 54, 2199–2211, 2018.
- 585 Dong, J., Ochsner, T. E., Zreda, M., Cosh, M. H., and Zou, C. B.: Calibration and validation of the COSMOS rover for surface soil moisture measurement, *Vadose Zone Journal*, 13, 1–8, 2014.
- Döpfer, V., Rocha, A. D., Berger, K., Gränzig, T., Verrelst, J., Kleinschmit, B., and Förster, M.: Estimating soil moisture content under grassland with hyperspectral data using radiative transfer modelling and machine learning, *International Journal of Applied Earth Observation and Geoinformation*, 110, 102817, 2022.
- 590 ESA: Global Land Cover Map for 2009, [http://due.esrin.esa.int/files/Globcover2009\\_V2.3\\_Global\\_.zip](http://due.esrin.esa.int/files/Globcover2009_V2.3_Global_.zip), last accessed on 1 June 2021, 2009.
- Foolad, F., Franz, T. E., Wang, T., Gibson, J., Kilic, A., Allen, R. G., and Suyker, A.: Feasibility analysis of using inverse modeling for estimating field-scale evapotranspiration in maize and soybean fields from soil water content monitoring networks, *Hydrology and Earth System Sciences*, 21, 1263–1277, <https://doi.org/10.5194/hess-21-1263-2017>, 2017.
- Franz, T., Zreda, M., Rosolem, R., and Ferre, T.: A universal calibration function for determination of soil moisture with cosmic-ray neutrons,  
595 *Hydrology and Earth System Sciences*, 17, 453–460, 2013.
- Franz, T. E., Zreda, M., Rosolem, R., and Ferre, T.: Field Validation of a Cosmic-Ray Neutron Sensor Using a Distributed Sensor Network, *Vadose Zone Journal*, 11, <https://doi.org/10.2136/vzj2012.0046>, 2012.
- Franz, T. E., Wahbi, A., Zhang, J., Vreugdenhil, M., Heng, L., Dercon, G., Strauss, P., Brocca, L., and Wagner, W.: Practical data products from cosmic-ray neutron sensing for hydrological applications, *Frontiers in Water*, 2, 9, 2020.
- 600 Fuamba, M., Branger, F., Braud, I., Batchabani, E., Sanzana, P., Sarrazin, B., and Jankowfsky, S.: Value of distributed water level and soil moisture data in the evaluation of a distributed hydrological model: Application to the PUMMA model in the Mercier catchment (6.6 km<sup>2</sup>) in France, *Journal of Hydrology*, 569, 753–770, 2019.

- Greacen, E. L.: Soil water assessment by the neutron method, CSIRO, Australia, 1981.
- 605 Gupta, H. V., Sorooshian, S., and Yapo, P. O.: Status of automatic calibration for hydrologic models: Comparison with multilevel expert calibration, *Journal of hydrologic engineering*, 4, 135–143, 1999.
- Gupta, H. V., Kling, H., Yilmaz, K. K., and Martinez, G. F.: Decomposition of the mean squared error and NSE performance criteria: Implications for improving hydrological modelling, *Journal of Hydrology*, 377, 80–91, 2009.
- Hargreaves, G. H. and Samani, Z. A.: Reference Crop Evapotranspiration from Temperature, *Applied Engineering in Agriculture*, 1, 96–99, <https://doi.org/10.13031/2013.26773>, 1985.
- 610 Hawdon, A., McJannet, D., and Wallace, J.: Calibration and correction procedures for cosmic-ray neutron soil moisture probes located across Australia, *Water Resources Research*, 50, 5029–5043, 2014.
- Heistermann, M., Francke, T., Schrön, M., and Oswald, S. E.: Spatio-temporal soil moisture retrieval at the catchment scale using a dense network of cosmic-ray neutron sensors, *Hydrology and Earth System Sciences*, 25, 4807–4824, 2021.
- Hermanns, F., Pohl, F., Rebmann, C., Schulz, G., Werban, U., and Lausch, A.: Inferring grassland drought stress with unsupervised learning 615 from airborne hyperspectral VNIR imagery, *Remote Sensing*, 13, 1885, 2021.
- Huang, S., Kumar, R., Flörke, M., Yang, T., Hundecha, Y., Kraft, P., Gao, C., Gelfan, A., Liersch, S., Lobanova, A., et al.: Evaluation of an ensemble of regional hydrological models in 12 large-scale river basins worldwide, *Climatic Change*, 141, 381–397, 2017.
- Iwema, J., Rosolem, R., Baatz, R., Wagener, T., and Bogena, H.: Investigating temporal field sampling strategies for site-specific calibration of three soil moisture–neutron intensity parameterisation methods, *Hydrology and Earth System Sciences*, 19, 3203–3216, 2015.
- 620 Iwema, J., Rosolem, R., Rahman, M., Blyth, E., and Wagener, T.: Land surface model performance using cosmic-ray and point-scale soil moisture measurements for calibration, *Hydrology and Earth System Sciences*, 21, 2843–2861, 2017.
- Jablonowski, C.: Adaptive grids in weather and climate modeling, University of Michigan, 2004.
- James, L. D.: Selection, calibration, and testing of hydrologic models, *Hydrologic modeling of small watersheds*, pp. 437–472, 1982.
- Jing, M., Heße, F., Kumar, R., Wang, W., Fischer, T., Walther, M., Zink, M., Zech, A., Samaniego, L., Kolditz, O., et al.: Improved regional- 625 scale groundwater representation by the coupling of the mesoscale Hydrologic Model (mHM v5. 7) to the groundwater model OpenGeoSys (OGS), *Geoscientific Model Development*, 11, 1989–2007, 2018.
- Kasner, M., Zacharias, S., and Schrön, M.: On soil bulk density and its influence to soil moisture estimation with cosmic-ray neutrons, *Hydrology and Earth System Sciences Discussions*, pp. 1–24, 2022.
- Koch, J., Demirel, M. C., and Stisen, S.: Climate normalized spatial patterns of evapotranspiration enhance the calibration of a hydrological 630 model, *Remote Sensing*, 14, 315, 2022.
- Köhli, M., Schrön, M., Zreda, M., Schmidt, U., Dietrich, P., and Zacharias, S.: Footprint characteristics revised for field-scale soil moisture monitoring with cosmic-ray neutrons, *Water Resources Research*, 51, 5772–5790, 2015.
- Köhli, M., Schrön, M., Zacharias, S., and Schmidt, U.: URANOS v1.0 – the Ultra Rapid Adaptable Neutron-Only Simulation for Environmental Research, *Geoscientific Model Development*, 16, 449–477, <https://doi.org/10.5194/gmd-16-449-2023>, 2023.
- 635 Kumar, R., Livneh, B., and Samaniego, L.: Toward computationally efficient large-scale hydrologic predictions with a multiscale regionalization scheme, *Water Resources Research*, 49, 5700–5714, 2013a.
- Kumar, R., Samaniego, L., and Attinger, S.: Implications of distributed hydrologic model parameterization on water fluxes at multiple scales and locations, *Water Resources Research*, 49, 360–379, 2013b.
- Köhli, M., Weimar, J., Schrön, M., Baatz, R., and Schmidt, U.: Soil Moisture and Air Humidity Dependence of the Above-Ground Cosmic- 640 Ray Neutron Intensity, *Frontiers in Water*, 2, 544 847, <https://doi.org/10.3389/frwa.2020.544847>, 2021.

- Liu, Y., Fernández-Ortega, J., Mudarra, M., and Hartmann, A.: Pitfalls and a feasible solution for using KGE as an informal likelihood function in MCMC methods: DREAM (ZS) as an example, *Hydrology and Earth System Sciences*, 26, 5341–5355, 2022.
- Livneh, B., Kumar, R., and Samaniego, L.: Influence of soil textural properties on hydrologic fluxes in the Mississippi river basin, *Hydrological Processes*, 29, 4638–4655, 2015.
- 645 Mai, J.: Ten strategies towards successful calibration of environmental models, *Journal of Hydrology*, p. 129414, <https://doi.org/10.1016/j.jhydrol.2023.129414>, 2023.
- Martinez, G. F. and Gupta, H. V.: Toward improved identification of hydrological models: A diagnostic evaluation of the “abcd” monthly water balance model for the conterminous United States, *Water Resources Research*, 46, 2010.
- Massoud, E. C., Xu, C., Fisher, R. A., Knox, R. G., Walker, A. P., Serbin, S. P., Christoffersen, B. O., Holm, J. A., Kueppers, L. M., Ricciuto, D. M., et al.: Identification of key parameters controlling demographically structured vegetation dynamics in a land surface model: CLM4.5 (FATES), *Geoscientific Model Development*, 12, 4133–4164, 2019.
- 650 McJannet, D., Franz, T., Hawdon, A., Boadle, D., Baker, B., Almeida, A., Silberstein, R., Lambert, T., and Desilets, D.: Field testing of the universal calibration function for determination of soil moisture with cosmic-ray neutrons, *Water Resources Research*, 50, 5235–5248, 2014.
- 655 McJannet, D., Hawdon, A., Baker, B., Renzullo, L., and Searle, R.: Multiscale soil moisture estimates using static and roving cosmic-ray soil moisture sensors, *Hydrology and Earth System Sciences*, 21, 6049–6067, <https://doi.org/10.5194/hess-21-6049-2017>, 2017.
- Moravec, V., Markonis, Y., Rakovec, O., Kumar, R., and Hanel, M.: A 250-year European drought inventory derived from ensemble hydrologic modeling, *Geophysical Research Letters*, 46, 5909–5917, 2019.
- OpenStreetMap contributors: Planet dump retrieved from <https://planet.osm.org> (last access: 26 July 2021), available at: <https://www.openstreetmap.org> (last access: 26 July 2021), a, b, c, 2020.
- 660 Patil, A., Fersch, B., Hendricks Franssen, H.-J., and Kunstmann, H.: Assimilation of cosmogenic neutron counts for improved soil moisture prediction in a distributed land surface model, *Frontiers in Water*, p. 115, 2021.
- Pohl, F., Rakovec, O., Rebmann, C., Hildebrandt, A., Boeing, F., Hermanns, F., Attinger, S., Samaniego, L., and Kumar, R.: Long-term daily hydrometeorological drought indices, soil moisture, and evapotranspiration for ICOS sites, *Scientific Data*, 10, 281, 2023.
- 665 Rakovec, O., Kumar, R., Attinger, S., and Samaniego, L.: Improving the realism of hydrologic model functioning through multivariate parameter estimation, *Water Resources Research*, 52, 7779–7792, 2016a.
- Rakovec, O., Kumar, R., Mai, J., Cuntz, M., Thober, S., Zink, M., Attinger, S., Schäfer, D., Schrön, M., and Samaniego, L.: Multi-scale and Multivariate Evaluation of Water Fluxes and States over European River Basins, *Journal of Hydrometeorology*, 17, 287–307, <https://doi.org/10.1175/jhm-d-15-0054.1>, 2016b.
- 670 Rakovec, O., Mizukami, N., Kumar, R., Newman, A. J., Thober, S., Wood, A. W., Clark, M. P., and Samaniego, L.: Diagnostic evaluation of large-domain hydrologic models calibrated across the contiguous United States, *Journal of Geophysical Research: Atmospheres*, 124, 13 991–14 007, 2019.
- Rakovec, O., Samaniego, L., Hari, V., Markonis, Y., Moravec, V., Thober, S., Hanel, M., and Kumar, R.: The 2018–2020 multi-year drought sets a new benchmark in Europe, *Earth’s Future*, 10, e2021EF002 394, 2022.
- 675 Rivera Villarreyes, C., Baroni, G., and Oswald, S. E.: Integral quantification of seasonal soil moisture changes in farmland by cosmic-ray neutrons, *Hydrology and Earth System Sciences*, 15, 3843–3859, 2011.
- Rivera Villarreyes, C. A., Baroni, G., and Oswald, S. E.: Inverse modelling of cosmic-ray soil moisture for field-scale soil hydraulic parameters, *European Journal of Soil Science*, 65, 876–886, <https://doi.org/10.1111/ejss.12162>, 2014.

- Rosolem, R., Hoar, T., Arellano, A., Anderson, J. L., Shuttleworth, W. J., Zeng, X., and Franz, T. E.: Translating aboveground cosmic-ray neutron intensity to high-frequency soil moisture profiles at sub-kilometer scale, *Hydrology and Earth System Sciences*, 18, 4363–4379, 2014.
- 680 Samaniego, L., Bárdossy, A., and Kumar, R.: Streamflow prediction in ungauged catchments using copula-based dissimilarity measures, *Water Resources Research*, 46, 2010a.
- Samaniego, L., Kumar, R., and Attinger, S.: Multiscale parameter regionalization of a grid-based hydrologic model at the mesoscale, *Water Resources Research*, 46, 2010b.
- 685 Samaniego, L., Kumar, R., and Zink, M.: Implications of parameter uncertainty on soil moisture drought analysis in Germany, *Journal of Hydrometeorology*, 14, 47–68, 2013.
- Samaniego, L., Kumar, R., Thober, S., Rakovec, O., Zink, M., Wanders, N., Eisner, S., Müller Schmied, H., Sutanudjaja, E. H., Warrach-Sagi, K., et al.: Toward seamless hydrologic predictions across spatial scales, *Hydrology and Earth System Sciences*, 21, 4323–4346, 2017.
- 690 Samaniego, L., Thober, S., Wanders, N., Pan, M., Rakovec, O., Sheffield, J., Wood, E. F., Prudhomme, C., Rees, G., Houghton-Carr, H., Fry, M., Smith, K., Watts, G., Hisdal, H., Estrela, T., Buontempo, C., Marx, A., and Kumar, R.: Hydrological Forecasts and Projections for Improved Decision-Making in the Water Sector in Europe, *Bulletin of the American Meteorological Society*, 100, 2451–2472, <https://doi.org/10.1175/bams-d-17-0274.1>, 2019.
- Samaniego, L., Kumar, R., Zink, M., Cuntz, M., Mai, J., Thober, S., Schneider, C., Dalmasso, G., Musuza, J., Rakovec, O., Craven, J., Schäfer, D., Prykhodko, V., Schrön, M., Spieler, D., Brenner, J., Langenberg, B., Schüler, L., Stisen, S., Demirel, C. M., Jing, M., Kaluza, M., Schweppe, R., Shrestha, P. K., Döring, N., and Müller, S.: mesoscale Hydrologic Model - mHM v5.13.0, Zenodo, <https://doi.org/10.5281/zenodo.7997974>, 2023.
- 695 Santanello Jr, J. A., Peters-Lidard, C. D., and Kumar, S. V.: Diagnosing the sensitivity of local land–atmosphere coupling via the soil moisture–boundary layer interaction, *Journal of Hydrometeorology*, 12, 766–786, 2011.
- 700 Scharnweber, T., Smiljanic, M., Cruz-García, R., Manthey, M., and Wilmking, M.: Tree growth at the end of the 21st century-the extreme years 2018/19 as template for future growth conditions, *Environmental Research Letters*, 15, 074 022, 2020.
- Schmidt, T., Schrön, M., Li, Z., Francke, T., Zacharias, S., Hildebrandt, A., and Peng, J.: Comprehensive quality assessment of satellite- and model-based soil moisture products against the COSMOS network in Germany, *Remote Sensing of Environment*, 301, 113 930, <https://doi.org/10.1016/j.rse.2023.113930>, 2024.
- 705 Schreiner-McGraw, A. P., Vivoni, E. R., Mascaro, G., and Franz, T. E.: Closing the water balance with cosmic-ray soil moisture measurements and assessing their relation to evapotranspiration in two semiarid watersheds, *Hydrology and Earth System Sciences*, 20, 329–345, <https://doi.org/10.5194/hess-20-329-2016>, 2015.
- Schreiner-McGraw, A. P., Vivoni, E. R., Mascaro, G., and Franz, T. E.: Closing the water balance with cosmic-ray soil moisture measurements and assessing their relation to evapotranspiration in two semiarid watersheds, *Hydrology and Earth System Sciences*, 20, 329–345, 2016.
- 710 Schrön, M.: Cosmic-ray Neutron Sensing and Its Applications to Soil and Land Surface Hydrology: On Neutron Physics, Method Development, and Soil Moisture Estimation Across Scales, Ph.D. thesis, Universität Potsdam, [https://publishup.uni-potsdam.de/files/39543/schroen\\_diss.pdf](https://publishup.uni-potsdam.de/files/39543/schroen_diss.pdf), 2017.
- Schrön, M., Köhli, M., Scheffele, L., Iwema, J., Bogena, H. R., Lv, L., Martini, E., Baroni, G., Rosolem, R., Weimar, J., et al.: Improving calibration and validation of cosmic-ray neutron sensors in the light of spatial sensitivity, *Hydrology and Earth System Sciences*, 21, 715 5009–5030, 2017.



- Schwepe, R., Thober, S., Müller, S., Kelbling, M., Kumar, R., Attinger, S., and Samaniego, L.: MPR 1.0: a stand-alone multiscale parameter regionalization tool for improved parameter estimation of land surface models, *Geoscientific Model Development*, 15, 859–882, 2022.
- Seneviratne, S. I., Lüthi, D., Litschi, M., and Schär, C.: Land–atmosphere coupling and climate change in Europe, *Nature*, 443, 205–209, 2006.
- 720 Shuttleworth, J., Rosolem, R., Zreda, M., and Franz, T.: The COsmic-ray Soil Moisture Interaction Code (COSMIC) for use in data assimilation, *Hydrology and Earth System Sciences*, 17, 3205–3217, 2013.
- Smith, K. A., Barker, L. J., Tanguy, M., Parry, S., Harrigan, S., Legg, T. P., Prudhomme, C., and Hannaford, J.: A multi-objective ensemble approach to hydrological modelling in the UK: an application to historic drought reconstruction, *Hydrology and Earth System Sciences*, 23, 3247–3268, 2019.
- 725 Van Steenberghe, N. and Willems, P.: Increasing river flood preparedness by real-time warning based on wetness state conditions, *Journal of Hydrology*, 489, 227–237, 2013.
- Vather, T., Everson, C., and Franz, T. E.: Calibration and validation of the cosmic ray neutron rover for soil water mapping within two South African land classes, *Hydrology*, 6, 65, 2019.
- Wahbi, A., Heng, L., and Dercon, G.: Cosmic ray neutron sensing: estimation of agricultural crop biomass water equivalent, *Springer Nature*, 730 2018.
- Wang, E., Smith, C. J., Macdonald, B. C., Hunt, J. R., Xing, H., Denmead, O., Zeglin, S., Zhao, Z., and Isaac, P.: Making sense of cosmic-ray soil moisture measurements and eddy covariance data with regard to crop water use and field water balance, *Agricultural Water Management*, 204, 271–280, <https://doi.org/10.1016/j.agwat.2018.04.017>, 2018.
- Warm Winter, W.: Warm Winter 2020 Team and ICOS Ecosystem Thematic Centre: Warm Winter 2020 ecosystem eddy covariance flux product for 73 stations in FLUXNET-Archive format–release 2022-1 (Version 1.0), ICOS Carbon Portal [data set], 735 <https://doi.org/10.18160/2G60-ZHAK>, 2022.
- Wollschläger, U., Attinger, S., Borchardt, D., Brauns, M., Cuntz, M., Dietrich, P., Fleckenstein, J. H., Friese, K., Friesen, J., Harpke, A., et al.: The Bode hydrological observatory: a platform for integrated, interdisciplinary hydro-ecological research within the TERENO Harz/Central German Lowland Observatory, *Environmental Earth Sciences*, 76, 1–25, 2017.
- 740 Zacharias, S. and Wessolek, G.: Excluding organic matter content from pedotransfer predictors of soil water retention, *Soil Science Society of America Journal*, 71, 43–50, 2007.
- Zacharias, S., Bogen, H., Samaniego, L., Mauder, M., Fuß, R., Pu<sup>o</sup>tz, T., Frenzel, M., Schwank, M., Baessler, C., Butterbach-Bahl, K., et al.: A network of terrestrial environmental observatories in Germany, *Vadose zone journal*, 10, 955–973, 2011.
- Zhao, H., Montzka, C., Baatz, R., Vereecken, H., and Franssen, H.-J. H.: The Importance of Subsurface Processes in Land Surface Modeling 745 over a Temperate Region: An Analysis with SMAP, Cosmic Ray Neutron Sensing and Triple Collocation Analysis, *Remote Sensing*, 13, 3068, 2021.
- Zheng, Y., Coxon, G., Woods, R., Power, D., Rico-Ramirez, M. A., McJannet, D., Rosolem, R., Li, J., and Feng, P.: Evaluation of reanalysis soil moisture products using cosmic ray neutron sensor observations across the globe, *Hydrology and Earth System Sciences*, 28, 1999–2022, <https://doi.org/10.5194/hess-28-1999-2024>, 2024.
- 750 Zhuo, L., Dai, Q., Zhao, B., and Han, D.: Soil moisture sensor network design for hydrological applications, *Hydrology and Earth System Sciences*, 24, 2577–2591, 2020.
- Zink, M., Samaniego, L., Kumar, R., Thober, S., Mai, J., Schäfer, D., and Marx, A.: The German drought monitor, *Environmental Research Letters*, 11, 074002, 2016.

- Zink, M., Kumar, R., Cuntz, M., and Samaniego, L.: A high-resolution dataset of water fluxes and states for Germany accounting for parametric uncertainty, *Hydrology and Earth System Sciences*, 21, 1769–1790, 2017.
- Zink, M., Samaniego, L., Kumar, R., Thober, S., Mai, J., Schäfer, D., and Marx, A.: A national scale planning tool for agricultural droughts in Germany, in: *Advances in chemical pollution, environmental management and protection*, vol. 3, pp. 147–169, Elsevier, 2018.
- Zreda, M.: Land-surface hydrology with cosmic-ray neutrons: Principles and applications, *Journal of the Japanese Society of Soil Physics*, 132, 25–30, 2016.
- 760 Zreda, M., Desilets, D., Ferré, T., and Scott, R. L.: Measuring soil moisture content non-invasively at intermediate spatial scale using cosmic-ray neutrons, *Geophysical research letters*, 35, 2008.
- Zreda, M., Shuttleworth, W., Zeng, X., Zweck, C., Desilets, D., Franz, T., and Rosolem, R.: COSMOS: The cosmic-ray soil moisture observing system, *Hydrology and Earth System Sciences*, 16, 4079–4099, 2012a.
- Zreda, M., Shuttleworth, W. J., Zeng, X., Zweck, C., Desilets, D., Franz, T., and Rosolem, R.: COSMOS: the COsmic-ray Soil Moisture  
765 Observing System, *Hydrology and Earth System Sciences*, 16, 4079–4099, <https://doi.org/10.5194/hess-16-4079-2012>, 2012b.